THE UNIVERSITY OF BRITISH COLUMBIA

FACULTY OF GRADUATE STUDIES

PROGRAMME OF THE FINAL ORAL EXAMINATION FOR THE DEGREE OF DOCTOR OF PHILOSOPHY

of

EDSEL KENNETH DARBY
B.Sc. (University of Saskatchewan) 1946
M.Sc. (University of Saskatchewan) 1948

THURSDAY, APRIL 24th, 1952, at 3:00 P.M.
IN ROOM 303 PHYSICS BUILDING

COMMITTEE IN CHARGE:

Dean H. F. Angus, *Chairman*

Professor W. Opechowski	Professor M. Kirsch
Professor G. M. Shrum	Dean Blythe Eagles
Professor J. B. Warren	Professor F. Noakes
Professor C. A. Barnes	Professor A. Earle Birney

LIST OF PUBLICATIONS

1) Negative Feedback. Dosage Rate Meter using a very small Ionization Chamber. H. E. Johns, E. K. Darby, J. J. S. Hamilton. American J. Roentgenology and Radium Therapy, **61,** 550 (1949).

2) Depth Dose Data and Isodose Distributions for Radiation from a 22 Mev Betatron. H. E. Johns, E. K. Darby, R. N. H. Hawlour, L. Katz and E. L. Harrington, American J. Roentgenology and Radium Therapy, **62,** 257 (1949).

3) Dosage Distributions Obtainable with 400 KVP X-rays and 22 Mev X-rays. H. E. Johns, E. K. Darby, I. A. Watson, C. C. Barkell. Br. J. Radiology, **23,** 290 (1950).

4) Depth Dose Distributions near Edge of X-ray Beam. H. E. Johns, E. K. Darby. Br. J. Radiology, **23,** 193 (1950).

5) A Radon Measuring Device. E. K. Darby, H. E. Johns. Am. J. Roentgenology and Radium Therapy, **64,** 472 (1951).

6) The Betatron in Cancer Therapy. H. E. Johns, E. K. Darby et al. Presented by H. E. Johns at 6th International Congress of Radiology, London, July 23 - 26, 1950.

7) Ultra-Violet Photon Counting with Electron Multiplier. G. W. Williams, A. H. Morrish and E. K. Darby. R.S.I., **21,** 884 (1950).

8) Energy Dependence of the Beta-Gamma Angular Correlation in Sb^{124}. E. K. Darby and W. Opechowski. Phys. Rev. **83,** 676 (1951).

9) Some Studies in Angular Correlation. E. K. Darby. Can. J. of Physics **29,** 569 (1951).

THESIS

SOME STUDIES IN BETA-GAMMA AND GAMMA-GAMMA ANGULAR CORRELATION

Abstract:

The beta-gamma angular correlation for Sb^{124} has been measured as a function of the beta particle energy in the range from 1.0 Mev to the end of the beta particle spectrum (2.4 Mev.). As a beta particle spectrometer, use was made of a twelve channel kicksorter and a thick crystal beta particle scintillation counter. This was connected in coincidence with a gamma ray scintillation counter. Accordingly, the beta gamma coincidence counting rate W (Θ, E), as a function of the angle Θ between the counters, and the energy E of the beta particles, was observed. The differential angular correlation coefficient

$$a\,(E) = \frac{W\,(180°,\,E) - W\,(90°,\,E)}{W\,(90°,\,E)}$$

was found to vary smoothly from -0.17 at 1.0 Mev to -0.44 at the end of the beta particle spectrum. When a (E) is integrated, numerically, over all beta particle energies greater than 1 Mev, the value of the integrated angular correlation coefficient $a = -0.24 \pm 0.02$ so obtained, agrees with the value $a = -0.23 \pm 0.01$ which was measured directly.

An attempt has been made to interpret these results in terms of the angular momenta of the particles emitted, using the theory developed by Falkoff and Uhlenbeck. Experiments on the gamma-gamma angular correlation of Co^{60} and Sc^{46} performed with the same apparatus are in agreement with the previous results of other workers.

GRADUATE STUDIES

Field of Study: Physics

Thermodynamics—Prof. C. A. McKay
Spectroscopy—Prof. W. Petrie
Electromagnetic Theory—Prof. L. Katz
Nuclear Physics—Prof. H. E. Johns
Quantum Mechanics—Prof. G. M. Volkoff
Theory of Measurements—Prof. A. M. Crooker
Radiation Theory—Prof. F. A. Kaempffer
Electronics—Prof. A. Van der Ziel
Special Relativity—Prof. W. Opechowski

Other Studies:

Advanced Differential Equations—Prof. T. E. Hull
Radiochemistry—Prof. M. Kirsch and Dr. K. Starke

SOME STUDIES IN BETA-GAMMA- AND GAMMA-GAMMA- ANGULAR CORRELATION

by

EDSEL KENNETH DARBY

A THESIS SUBMITTED IN PARTIAL FULFILMENT OF THE REQUIREMENTS FOR THE DEGREE OF DOCTOR OF PHILOSOPHY

in

PHYSICS

We accept this thesis as conforming to the standard required from candidates for the degree of DOCTOR OF PHILOSOPHY.

Members of the Department of Physics.

THE UNIVERSITY OF BRITISH COLUMBIA

April, 1952.

ABSTRACT

The beta-gamma angular correlation for Sb^{124} has been measured as a function of the beta particle energy in the range from 0.82 Mev to the end of the beta particle spectrum (2.4 Mev). As a beta particle spectrometer, use was made of a twelve channel kicksorter and a thick crystal beta particle scintillation counter. This was connected in coincidence with a gamma ray scintillation counter. Accordingly, the beta gamma coincidence counting rate $W(\theta,E)$, as a function of the angle θ between the counters, and the energy E of the beta particles, was observed. The differential angular correlation coefficient:

$a(E)=\left[\frac{W(180^\circ,E) - W(90^\circ,E)}{W(90^\circ,E)}\right]$ was found to vary smoothly from -0.17 at 1.0 Mev to -0.44 at the end of the beta particle spectrum. When $a(E)$ is integrated, numerically, over all beta particle energies greater than 0.82 Mev., the value of the integrated angular correlation coefficient $a = -0.24 \pm 0.02$ was found. Direct measurements of the value of the integrated angular correlation coefficient were also performed, and the relation to the above value of a considered.

An attempt has been made to interpret these results in terms of the angular momenta of the particles emitted, using the theory developed by Falkoff and Uhlenbeck. Experiments on the gamma-gamma angular correlation of Co^{60} and Sc^{46} performed with the same apparatus are in agreement with the previous results of other workers.

TABLE OF CONTENTS

TABLE OF APPENDICES

TABLES

FIGURES

ACKNOWLEDGEMENTS

I am indebted to Professor W. Opechowski for valuable discussions in the course of these experiments, and for help in interpreting the experimental results. I am also indebted to Dr. A. H. Morrish for his suggestions in the early stages of the gamma-gamma correlation experiments and to Mr. G. W. Williams for his assistance in design and construction of the apparatus. I also wish to acknowledge the kind assistance of other staff members of the Physics Department and the excellent laboratory facilities supplied by the University of British Columbia Physics Department. This research was made possible by a grant from the National Research Council of Canada, and the author was aided by a Fellowship from the National Research Council of Canada.

I

INTRODUCTION.

The emission of a beta particle from a radioactive nucleus often leaves the product nucleus in an excited state. The excited nucleus may then decay, by the emission of one or more gamma rays in cascade, to the ground state. The disintegration scheme of Co^{60} (Fig. 1A) is a simple example of two gamma rays in cascade. The lifetime of the intermediate excited states is in general very small (10^{-12} sec.) so the two gamma rays may be regarded as simultaneous for most purposes. If we arrange two gamma ray counters near the Co^{60} source (Fig. 2) and connect them to a circuit designed to register two simultaneous pulses (coincidence circuit), we will be able to obtain a double coincidence counting rate. This coincidence rate is much smaller than the single counting rate in either counter since the probability of counting both gamma rays simultaneously is small. If, instead of having two gamma rays in cascade, we have only one gamma ray following the emitted beta particle (Fig. 1B), we can obtain coincidence counts by using one beta particle counter and one gamma counter.

Now the atoms in the radioactive source* are in this case randomly oriented so in the double-gamma cascade the first gamma-ray in the cascade is emitted in an entirely random

---

*The lifetime of the initial state must be long enough for the angular momentum vectors of the nuclei to become randomly oriented, either by precession in a magnetic field due to orbital electrons or by thermal agitation.

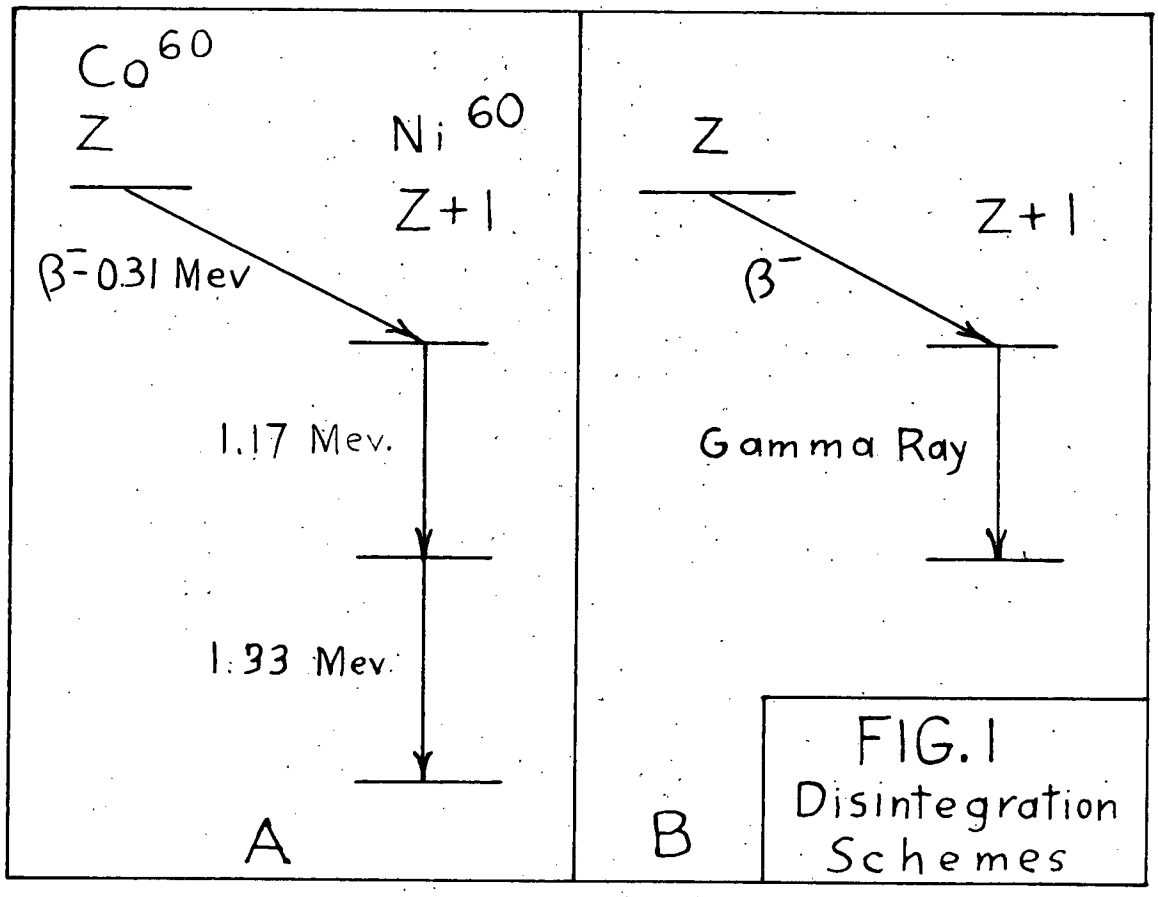

FIG. 1
Disintegration Schemes

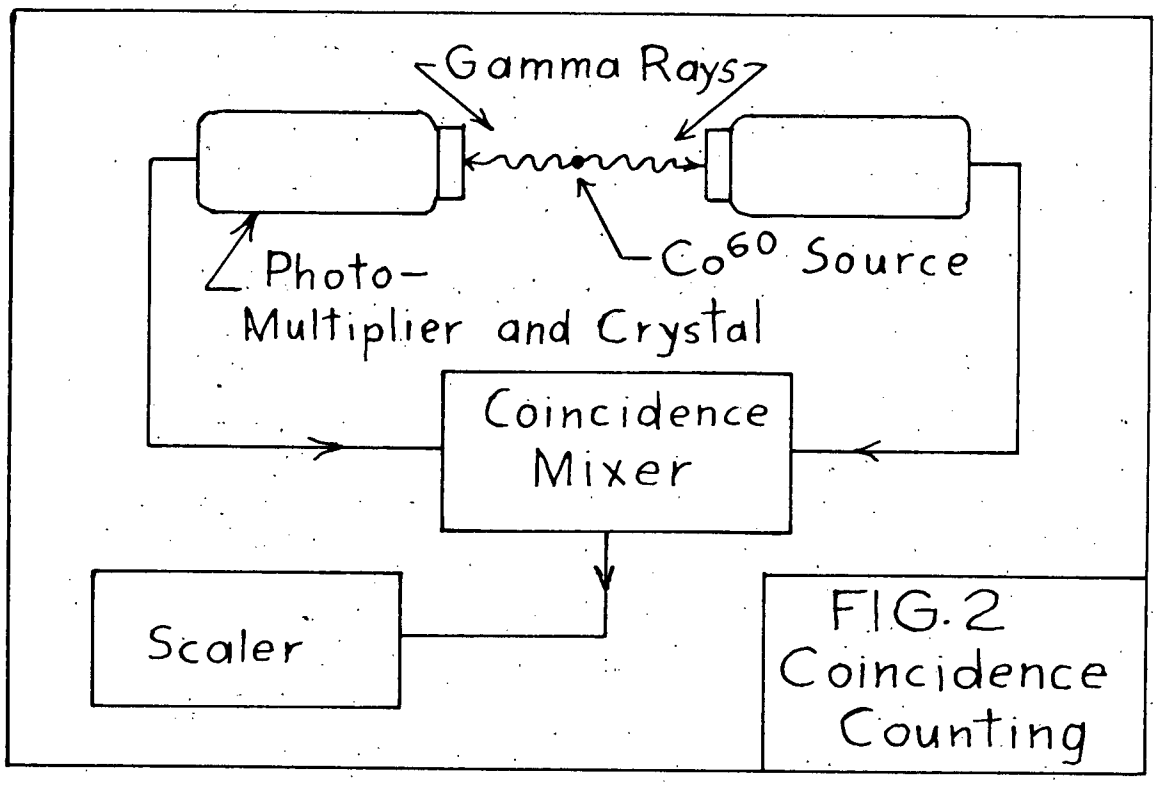

FIG. 2
Coincidence Counting

direction, however the second gamma-ray in some cases may have its direction of emission correlated with respect to the direction of emission of the first gamma-ray. This effect is called the angular correlation between the directions of the two gamma rays, or more briefly, gamma-gamma angular correlation. We can measure this gamma-gamma angular correlation by observing the gamma-gamma coincidence rate as a function of Θ, the angle between the counters. The gamma-gamma coincidence rate as a function of Θ(after a small correction for finite counter size) is proportional to the gamma-gamma angular correlation function, $W(\Theta)$, which is the probability of the emission of the second gamma ray in direction Θ with respect to the first gamma-ray's direction of emission.

In a similar manner if we observe the beta-gamma coincidence rate we sometimes observe a beta-gamma-angular correlation. The researches described in this thesis concern the beta-gamma- and gamma-gamma- angular correlation observed in several radioactive nuclei.

As an example of the information which is available from these experiments, let us consider the case of the gamma-gamma angular correlation in more detail. Gamma ray transitions are classified on the basis of the angular momentum carried away by the gamma ray. The multipole order of the transition is 2^L where L is the z-component of the angular momentum carried away by the gamma ray. Thus if the gamma ray has angular momentum $L=1$ (in units of $\hbar$), the transition is classified as dipole. The transitions are classified further according to whether or not there is a change of parity, that is whether or not there is

a change in the symmetry properties of the wave-functions of the two levels. In the case of dipole radiation if the parity changes the transition is called electric dipole, if it does not change, it is called magnetic dipole. If we consider only the case of "pure" multipole transitions (that is only one angular momentum associated with a given transition) then the theory indicates that the form of the angular-correlation function is as follows:

$$W(\theta) = 1 + \sum_{i=1}^{l} a_i \cos^{2i}\theta ,$$

where 2^l is the lowest multipole order of the two transitions. The coefficients a_i are functions of the multipole orders of the transitions, and of the angular momenta of the nuclear levels involved in the transitions. For many cases tables (2) have been prepared which give numerical values for the a_i. Experimentally, we can determine $\sum a_i$ quite accurately, and the values of the individual a_i approximately. If we have available some other information concerning either the angular momentum of the levels or the multipole order of the transitions, we can compare the experimental data with the tables, and usually obtain a definite assignment of angular momentum and multipole orders to the levels and transitions involved.

As an example of the procedure in interpretation of the data let us consider the case of Co^{60}. The measurements for Co^{60} give the correlation coefficient $\sum a_i = +0.157 \pm 0.01$. Moreover from the graph (Fig. 8) of the correlation function we see that the function is probably of the form:

$$W(\theta) = 1 + a_1 \cos^2\theta + a_2 \cos^4\theta .$$

Although the accuracy of the results does not permit us to

determine a_1, a_2 separately, the fact that there is a term in $\cos^4\theta$ means that both transitions are of at least quadrupole order. We have one other piece of information, namely that the angular momentum of the ground state is probably 0, since the product nucleus Ni^{60} has an even number of both protons and neutrons. The tables may now be searched quite quickly and it is seen that the correlation function for the double transition* $4 \xrightarrow{2} 2 \xrightarrow{2} 0$ is $W(\theta) = 1 + 0.125 \cos^2\theta + 0.040 \cos^4\theta$. This gives $\sum a_i = a_1 + a_2 = +0.165$ in quite close agreement with the experimental value 0.157 ± 0.010. We conclude therefore that the angular momenta and multipole orders for the transition involved are very likely to be given by the following scheme $4 \xrightarrow{2} 2 \xrightarrow{2} 0$.

The results for beta-gamma angular correlation may be interpreted in a similar fashion, leading to information

*The angular momentum of a nuclear state is often referred to as the "spin". Where no confusion should arise the term spin will be used for the sake of brevity. The transition scheme $4 \xrightarrow{2} 2 \xrightarrow{2} 0$. is to be interpreted as follows: the initial state has a spin of 4 (in units of $\hbar$), and a transition takes place to an intermediate state having spin 2. This transition is accompanied by a gamma ray having angular momentum 2 so it is classified as quadrupole. A transition then takes place from the intermediate state to the ground state with spin 0, this transition also being classified as quadrupole.

regarding the spins of the levels involved, the multipole orders of the gamma transition.

The original suggestion that gamma-gamma-angular correlation might exist was due to Dunworth (1); Following this suggestion, Hamilton (2) in 1940 presented the theory of the effect giving the results that have just been outlined. Attempts (3) (4) to detect an angular correlation failed and it was not until 1948 when Brady and Deutsch (5) reported the successful detection of a gamma-gamma angular correlation in four nuclei. Their success was due largely to the development of highly efficient gamma counters using crystal phosphors and photo-multipliers. During 1949 and 1950 numerous observers (6)(7)(8) reported confirmation of these results and new results for other nuclei. Further details of the theory had also been given by Goertzel (9) (effect of an external magnetic field), and Ling and Falkoff (10) (effect of "mixed" multipole transitions).

Although many nuclei have exhibited a gamma-gamma-angular correlation, numerous attempts to detect a beta-gamma-angular correlation resulted in failure, (11)(6)(13)(14). By 1951 only two nuclei (Sb^{124}, Rb^{86}) had yielded a definite beta-gamma-angular correlation (11)(12)(13), moreover the results reported were not consistent. Sufficient theory to allow a reasonable interpretation of results in most cases had been developed in 1950 by Falkoff and Uhlenbeck (15). Further investigation into the beta-gamma-angular correlation effect was required.

The main original contributions of the researches described in this thesis are the experiments on the beta-gamma-angular correlation in Sb^{124}. In particular since the beta

particles have a continuous energy distribution, the dependence of the angular correlation on the energy of the beta particles was the object of this investigation. Such an energy dependence was predicted theoretically by Falkoff and Uhlenbeck (15) but had not been observed previous to this in a quantitative way. The results of this investigation have been published, first in a preliminary report (16) and later in a full paper (17). Similar results have later been published by Stevenson and Deutsch (18) who used an entirely different experimental method, the agreement with the present work being quite good.

The gamma-gamma correlation experiments were not new, Brady and Deutsch (5) having observed this previously. However the accuracy obtained in the present work is somewhat better than in the previous work. Moreover, the same apparatus was employed later in the beta-gamma correlation experiments, so the consistency of the gamma-gamma correlation experiments lends support to the subsequent beta-gamma correlation results.

II.

THEORY OF GAMMA-GAMMA-ANGULAR CORRELATION.

The theory of directional correlation between successively emitted nuclear particles has been developed in considerable detail in several papers, (2)(9)(10). The problem involves the determination of $W(\theta)$, the relative probability of the emission of particle 2 in direction $\vec{k}_2$ following the emission of particle 1 in direction $\vec{k}_1$, the angle between $\vec{k}_1$ and $\vec{k}_2$ being θ and the transition taking place from $A \longrightarrow B$, $B \longrightarrow C$ as shown in Fig. 3.

Hamilton (2) has applied second order time dependent perturbation theory to the gamma-gamma problem and obtained $W(\theta)$ in terms of the spins of the nuclear states involved and angular momenta of the emitted photons. Hamiltons theory involves two assumptions, namely:

1. That the lifetime of the intermediate state is short compared with the nuclear precessional period.
2. That the transitions are "pure" multipole transitions and not due to a mixture of multipoles.

Goertzel (9) has extended Hamilton's theory to cover the case in which there is a strong magnetic field present so that the first assumption above is not fulfilled. Ling and Falkoff (10) have extended the theory to take into account mixtures of multipoles.

Falkoff and Uhlenbeck (15) have generalized Hamilton's theory (still retaining his assumptions however) and obtained $W(\theta)$ in parametric forms for arbitrary emitted particles. Specification of the types of emitted particles determines the parameters and gives $W(\theta)$ for the required type of correlation.

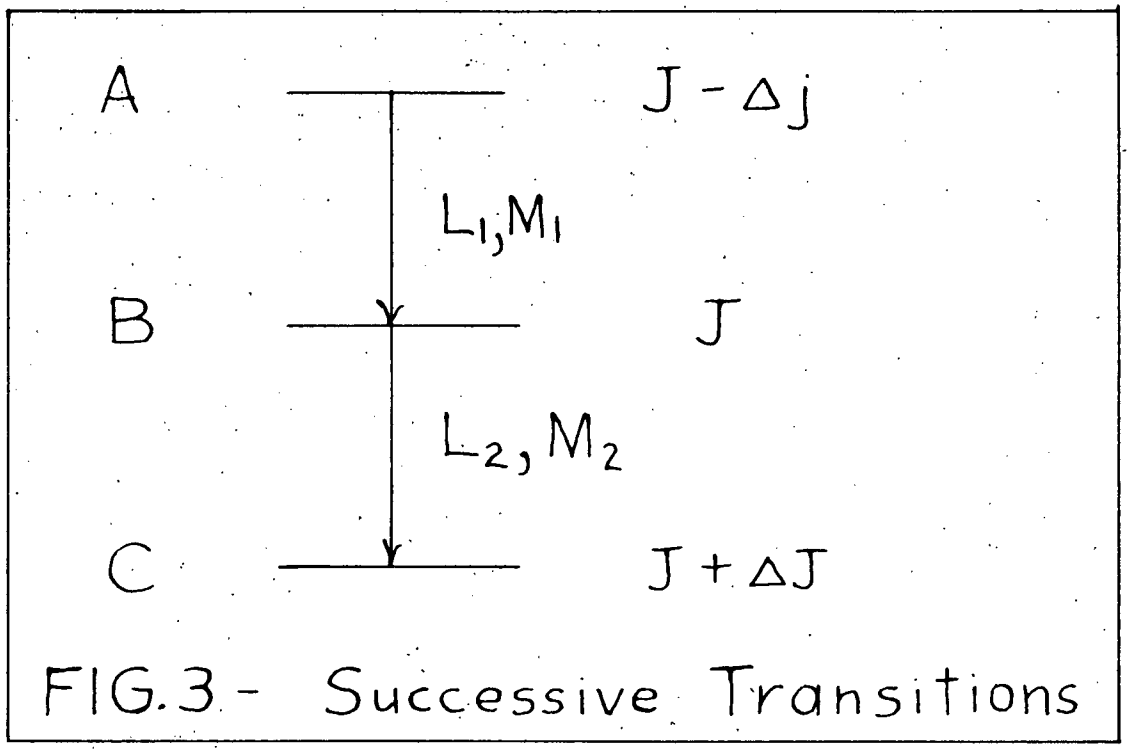

FIG. 3 - Successive Transitions

Choosing $\vec{k}_1$ as the axis of quantization the general result of the theory (2) (15) is:

$$W(\theta) = \sum_m \left\{ \sum_\ell \left[S_1 \left| (A_\ell \left| H_1(0) \right| B_m) \right|^2 \right] \right. \qquad (1)$$
$$\left. \times \sum_p \left[S_2 \left| (B_m \left| H_2(\theta) \right| C_p) \right|^2 \right] \right\} ,$$

where $(B_m | H_2(\theta) | C_p)$ denotes the matrix element of the Hamiltonian describing the interaction of the second emitted particle and the nucleus for the transition from the substate m of the (nuclear) state B (a state as characterized by a definite value of the total angular momentum quantum number) to the substate p of the state C. The meaning of $(A_\ell | H_1(0) | B_m)$ is of course similar. S_1 represents the average overall directional information (spins, polarization) for the first transition except of course the direction $\vec{k}_1$ with a similar meaning for S_2. The quantity:

$$S_1 \left| (A_\ell \left| H_1(0) \right| B_m) \right|^2 \equiv P_{\ell m}(0) , \qquad (2)$$

is the probability of the emission of the first particle along the axis of quantization for the transition between sublevels $A_\ell \rightarrow B_m$. $P_{mp}(\theta)$ is defined similarly so that $W(\theta)$ is given by:

$$W(\theta) = \sum_{\ell m p} P_{\ell m}(0) \cdot P_{mp}(\theta) . \qquad (3)$$

In general considering a transition between states with total and z component angular momenta J, m and $J' m'$ respectively and the emission of a particle having angular momentum quantum numbers L and M, group theoretical methods show that

$$P_{m m'}(\theta) = S\left|(B_m|H|C_{m'})\right|^2, \qquad (4)$$

can be written

$$P_{m m'}(\theta) = G_{m m'}^{J L J'} \cdot F_L^M(\theta) \qquad (5)$$

with $m' = m + M$ and $J' = J + L$.

Where the $G_{m m'}^{J L J'}$ when evaluated yield numerical values depending only upon these angular momenta, and not upon the kind of particle emitted and the $F_L^M(\theta)$ are the angular distributions which depend on the type of particle emitted. It turns out that if all the initial sublevels are equally populated, and the direction of emission of the particle is specified, then the intermediate sublevels will in general not be equally populated. Since the intermediate sublevels are not equally populated, the second particle will not likely have an isotropic distribution, thus exhibiting an angular correlation.

The $F_L^M(\theta)$ may be expressed in suitable parqmetric forms, in this case powers of $\cos^2\theta$. The maximum number of independent parameters is L. Falkoff and Uhlenbeck (15) obtain several convenient parametric forms. The parameters are specified according to the type of particle emitted. It is then only necessary to evaluate the $G_{m m'}^{J L J'}$ which are independent of the type of particle emitted, and then to obtain the $W(\theta)$ as in formula (3). The required sums have been evaluated by Hamilton (2) and are listed by Falkoff and Uhlenbeck (15) for $L = 1$ or 2. For higher values of angular momentum quantum numbers (of the nuclear states and the emitted particles) the computations of these sums become very difficult, and they have

been evaluated only for a certain number of special cases. For example Lloyd (19) and Hess (20).

The gamma-gamma angular correlation functions have been tabulated in a "canonical form" by Hamilton (2). That is, he writes the correlation function in the form:

$$W(\theta) = 1 + \frac{R}{Q} \cos^2\theta + \frac{S}{Q} \cos^4\theta ,$$

and gives tables of R, Q and S as functions of the angular momenta involved.

The same results may be obtained readily from the tables of Falkoff and Uhlenbeck (15) by inserting the proper parameters for the gamma-gamma transitions.

The following general results of the theory for gamma-gamma correlation may be listed:

1. The correlation function is of the form : $W(\theta) = 1 + \sum_{i=1}^{L} a_i \cos^{2i}\theta ,$ where L is the minimum of L_1, L_2.

2. The coefficients a_i depend on the angular momenta of the three levels and on the multipole order of the transition but not on parity change.

3. The highest power of $\cos^2\theta$ cannot exceed $2J$ so there is no correlation if the intermediate state has a spin of 0, or $\frac{1}{2}$.

III.

GAMMA-GAMMA-ANGULAR CORRELATION IN Co^{60} AND Sc^{46}.

The disintegration scheme of Co^{60} which consists of a 0.31 Mev beta group followed by cascade gamma rays of energies 1.17 Mev and 1.33 Mev is given in Fig. 1 (21). Sc^{46} has a similar decay scheme, (21), with a maximum beta particle energy of 0.36 Mev, and cascade gamma rays with energies of 0.88 Mev and 1.12 Mev respectively.

The Co^{60} source consisted of a wire of cobalt metal about 0.1 mm in diameter and 4 mm in length which had been irradiated in the Chalk River pile to an activity of about 300 μ curies. The source was supported vertically and enclosed in a sufficient thickness of aluminium to stop all Co^{60} beta particles. The Sc^{46} source consisted of Sc_2O_3 in an aluminium capsule.

The gamma counters employed 1 x 1 x $\frac{1}{2}$ in. anthracene crystals cemented to RCA-5819 photomultipliers with Canada balsam. The crystals were covered with a 0.001 in. thick aluminium foil as a light reflector. The counters were mounted on a spectrometer table, the general arrangement being as shown in Fig. 4. The source was rigidly supported and accurately centred on a thin aluminium rod machined to fit the hole in the centre of the spectrometer table. The electronics arrangement is shown in Fig. 5 with the detailed circuits being given in Appendix IX. The resolving time of the coincidence mixer is 0.18 μ-sec. The angular resolution of the counters was measured using annihilation radiation from a Cu^{64} source. An angle of 20° subtended by the counter at the source was selected as giving a sufficient counting rate, without requiring too large a correction

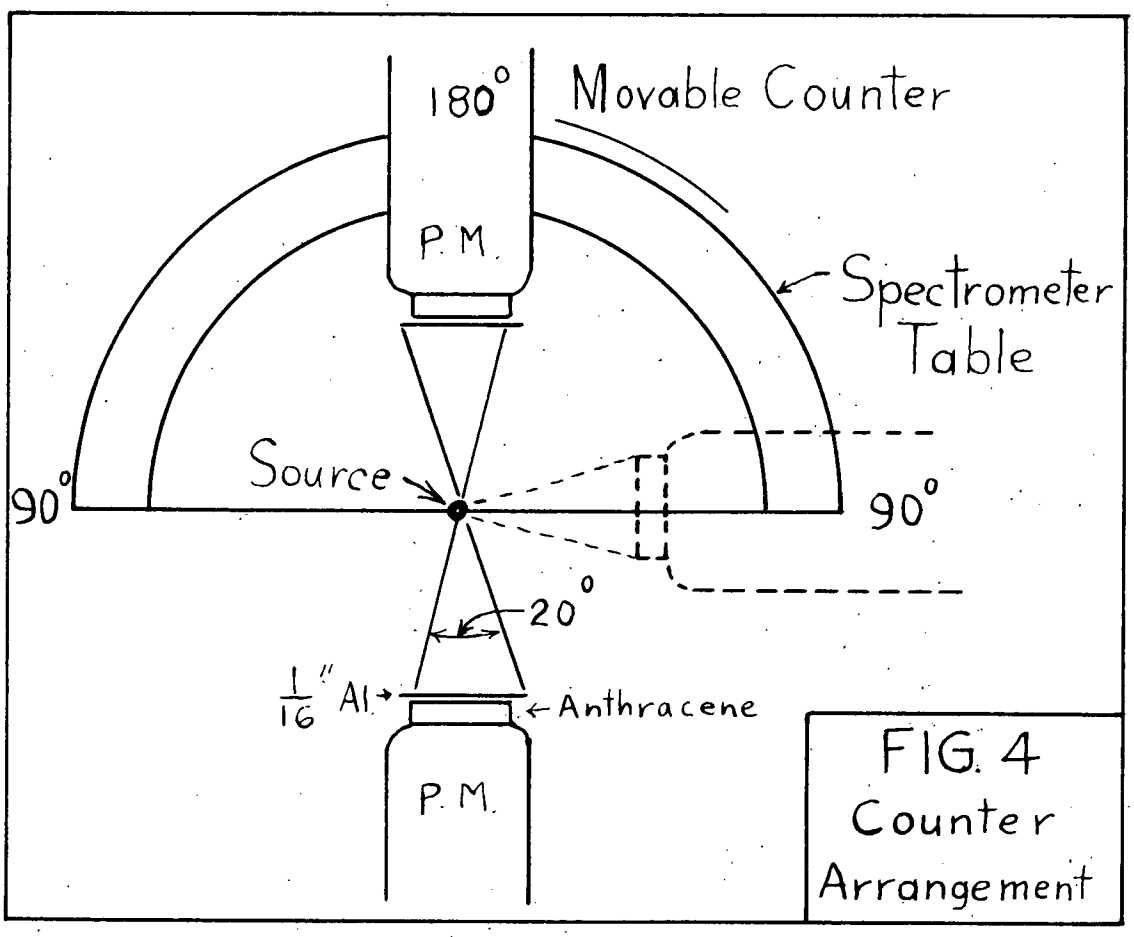

FIG. 4
Counter Arrangement

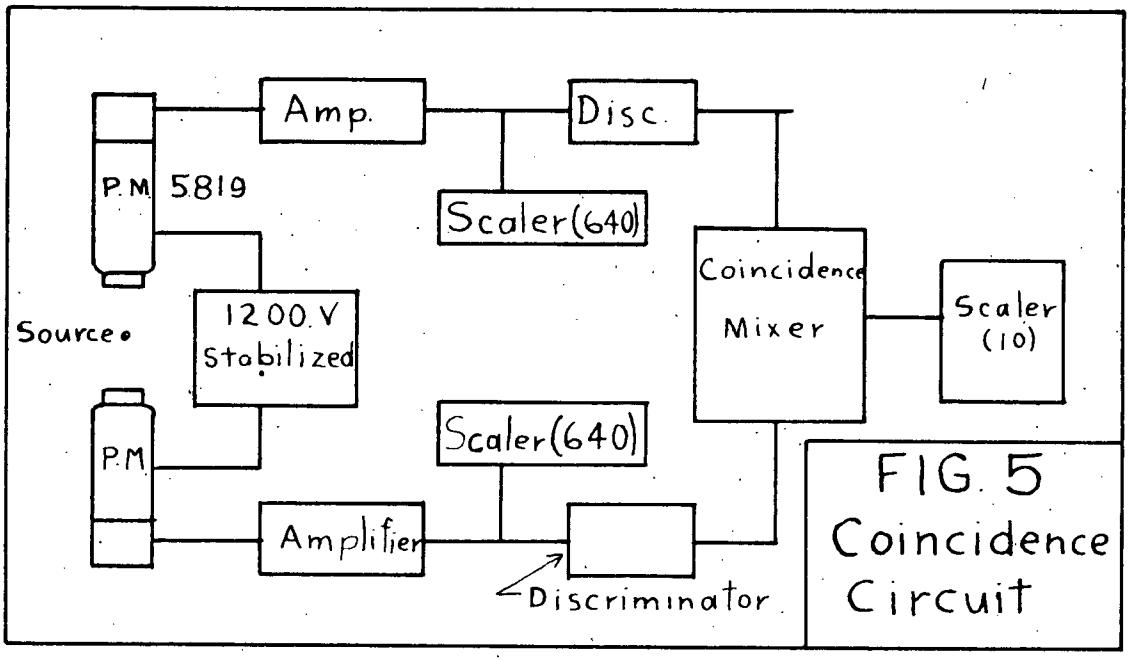

FIG. 5
Coincidence Circuit

for angular resolution.

The true angular correlation between the gamma rays may be masked by three spurious effects. These are as follows:

1. Compton scattering in one counter produces a lower energy gamma ray which may be counted in the second counter. Since the Compton scattering produces a count in the first counter, the above process results in a coincidence count. For the case of two 1 Mev gamma rays in cascade, a calculation (See Appendix III) shows that the coincidence counts so produced, which we call the "scattered coincidence rate", will be about 50% of the true coincidence rate, if we assume equal counting efficiencies for both the 1 Mev gamma ray and the gamma ray scattered through 180°. With the foregoing assumptions the ratio of scattered to true coincidence rate when the counters are placed at 90° will increase, because the solid angle between the counters is increased, although the number of scattered gammas per solid angle is slightly decreased.

This scattering from one counter to the other may be prevented by means of lead shielding such as is shown in Fig. 6. The source is placed in front of the aperture in the lead shield and the scattering is reduced directly in the proportion of the area of the aperture to the area of the counter crystal. In this way it was possible to reduce the scattered coincidence rate to $\frac{1}{100}$ of its value without a shield. This method is particularly suited to low energy gamma rays, i.e. 500 Kev or less, in which case the scattered gamma ray is not appreciably lower in energy. For gamma rays of the order of 1 Mev, the backward scattered gamma ray is about 200 Kev, so in this case it is simpler to merely discriminate against the 200 Kev pulses, the 1 Mev gamma rays

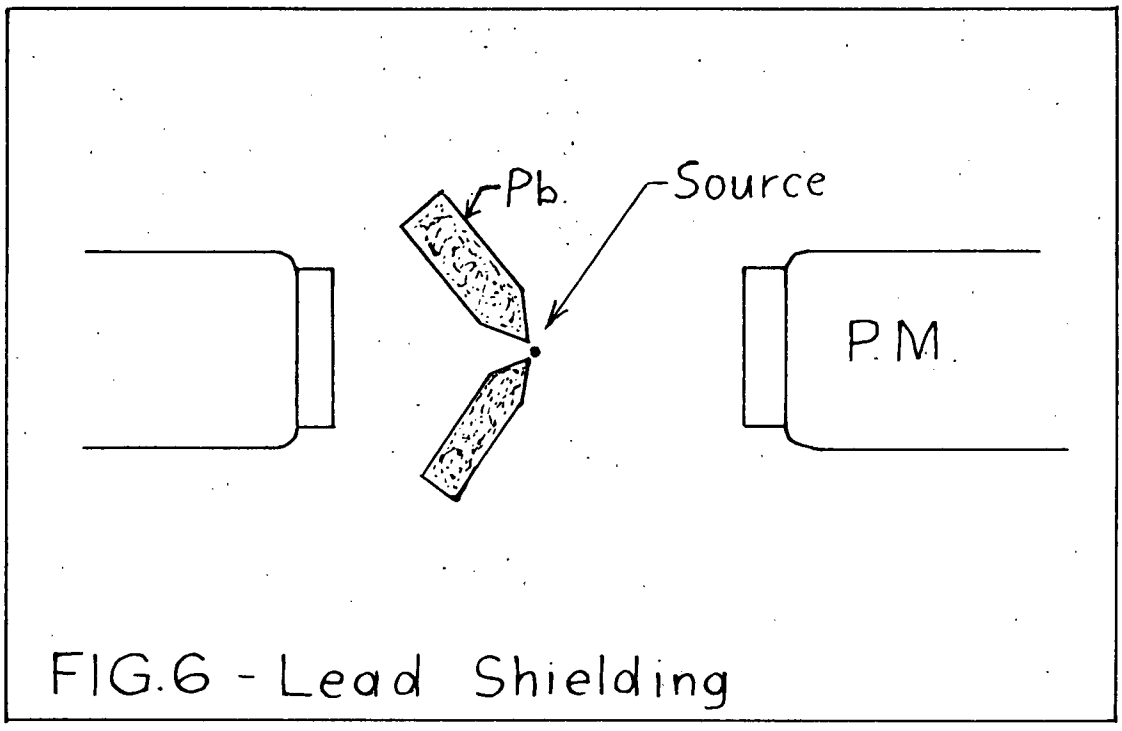

FIG.6 - Lead Shielding

being counted with only slightly reduced efficiency.

2. Compton and photo electrons may be ejected from the lead shielding if it is used. Owing to the relatively high efficiency of the counters for counting beta particles, the counting rate due to this scattering may be large compared with the gamma counting rate. This effect results mainly in changing the effective solid angle of the counters so its presence is undesirable. It may easily be eliminated by placing sufficient aluminium in front of the counters to stop photo electrons from the gamma rays in question.

3. For gamma rays of energy greater than 1.02 Mev, lead shielding cannot be used with confidence since pair production is then possible and the resulting annihilation radiation is strongly correlated. For example with the shielding arrangement shown in Fig. 6 and a Co^{60} source (gamma energies: 1.17 and 1.33 Mev), the correlation curve B shown in Fig. 7 was obtained. With the bias of the discriminators set to eliminate pulses corresponding to gamma rays below 250 Kev and no lead shielding in place, the curve A shown in Fig. 7 was obtained. The curves coincide up to about 160° and the sharp rise in curve B from 160° to 180° is characteristic of that produced by annihilation radiation with the counters set to subtend an included angle of 20°.

It was concluded from the preceding investigation that the most satisfactory method of avoiding spurious effects in measuring the angular correlation in Co^{60} and Sc^{46} was to discriminate against Compton scattered gamma ray pulses. Accordingly the discriminators were calibrated using the Co^{60} 1.3 Mev gamma pulses, and set to eliminate pulses corresponding to energies of less than 250 Kev. The only shielding employed was $\frac{1}{16}$" of aluminium

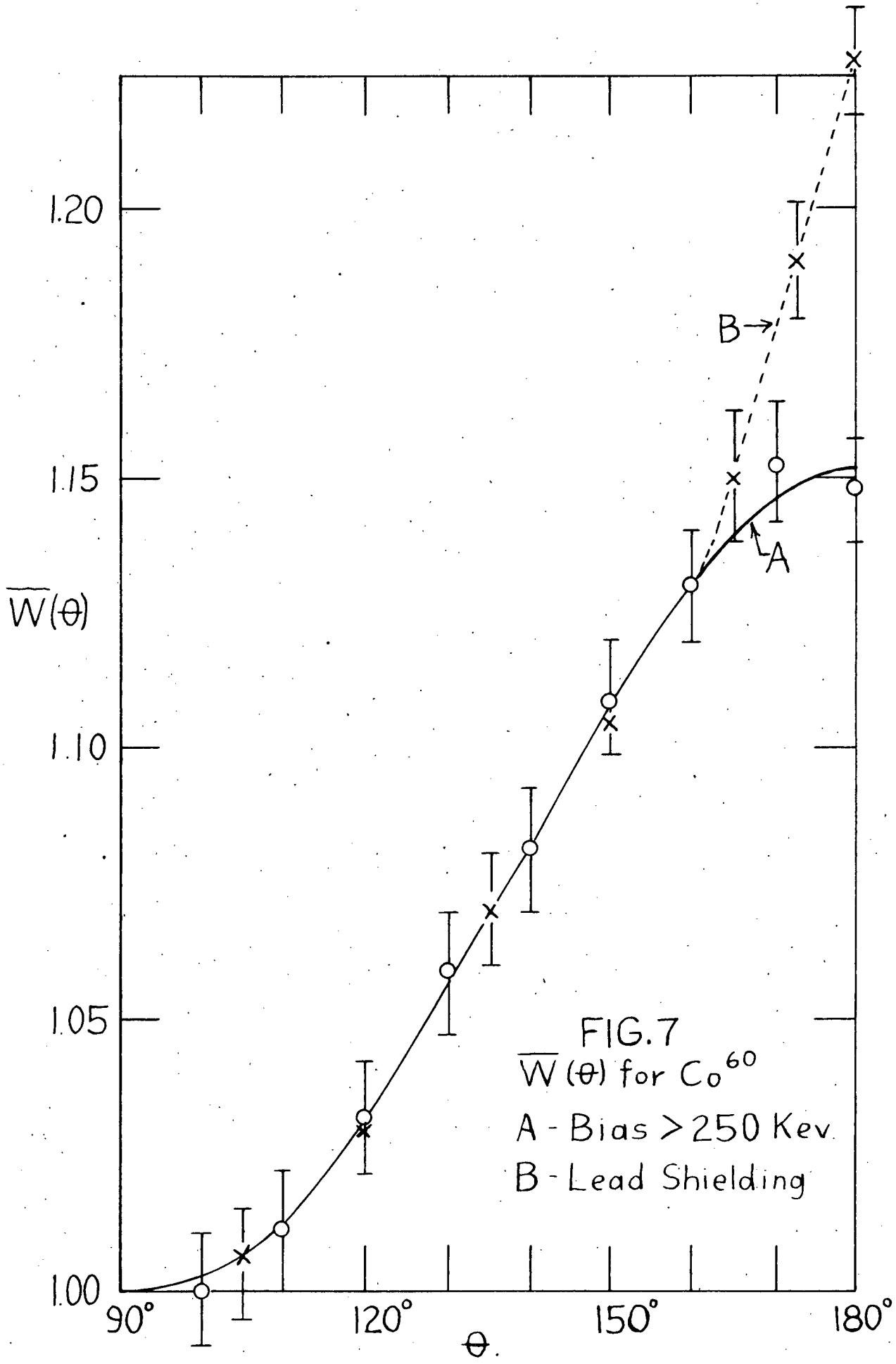

FIG. 7
$\overline{W}(\theta)$ for Co^{60}
A - Bias > 250 Kev.
B - Lead Shielding

immediately in front of each counter to stop beta particles.

The following procedure has been adopted in the evaluation of the experimental data:

1. The data recorded consisted of the time T (hours), the total coincidence counts $C(\theta)$, and the total single channel counts (scaled by 640) A and B.

2. Since the counter efficiencies may vary slightly (due to H.T. variations or moving one counter), the coincidence rate was divided by the individual channel counting rates to correct for these slight variations. Upon subtracting the accidental coincidence rate, calculated in the usual manner, we obtain the quantity:

$$C_T(\theta) = \left(\frac{CT}{AB} - 2\tau\right) \times 10^7 \qquad \text{where} \quad 2\tau = 407 .$$

The details are given in Appendices I and II.

3. The uncorrected correlation function, $\overline{W(\theta)} = \frac{C_T(\theta)}{C_T(90°)}$ was next evaluated.

4. $\overline{W(\theta)}$ was corrected for angular resolution by the method outlined in Appendix II to obtain the true angular correlation function, $W(\theta)$.

5. The standard deviation was calculated statistically on the basis of the number of counts obtained, (see Appendix IV).

6. A comparison was made with the theoretical values for $W(\theta)$ calculated from Hamilton's tables (2).

The evaluation of the experimental data is shown in Tables I and II for Co^{60} and Sc^{46} respectively. The corrected points ($W(\theta)$) are plotted in Figs. 8 and 9 for Co^{60}

TABLE I

Gamma-Gamma Angular Correlation in Co^{60}

θ	$C_T(\theta)$	$\bar{W}(\theta) - 1$	$W(\theta) - 1$	S.D.	$W(\theta)$ (Theoretical)
90°	967	0.000	0.000	0.000	1.000
100°	967	0.000	0.000	0.010	1.003
110°	973	0.011	0.012	0.012	1.014
120°	985	0.032	0.034	0.011	1.035
130°	1000	0.059	0.062	0.011	1.062
140°	1012	0.081	0.085	0.012	1.089
150°	1028	0.109	0.114	0.010	1.117
160°	1040	0.130	0.136	0.010	1.142
170°	1053	0.153	0.159	0.012	1.158
180°	1049	0.147	0.153	0.010	1.165

TABLE II

Gamma-Gamma Angular Correlation in Sc^{46}

θ	$C_T(\theta)$	$W(\theta)-1$	$W(\theta)-1$	S.D.	$W(\theta)$ Theoretical.
90°	623	0.000	0.000	0.000	1.000
100°	627	0.006	0.007	0.012	1.003
110°	635	0.019	0.020	0.010	1.014
120°	641	0.029	0.031	0.010	1.035
130°	652	0.047	0.049	0.011	1.062
140°	666	0.069	0.073	0.011	1.089
150°	682	0.095	0.099	0.008	1.117
160°	696	0.121	0.127	0.010	1.142
170°	710	0.140	0.146	0.008	1.158
175°	713	0.145	0.151	0.010	1.163
180°	718	0.152	0.158	0.009	1.165

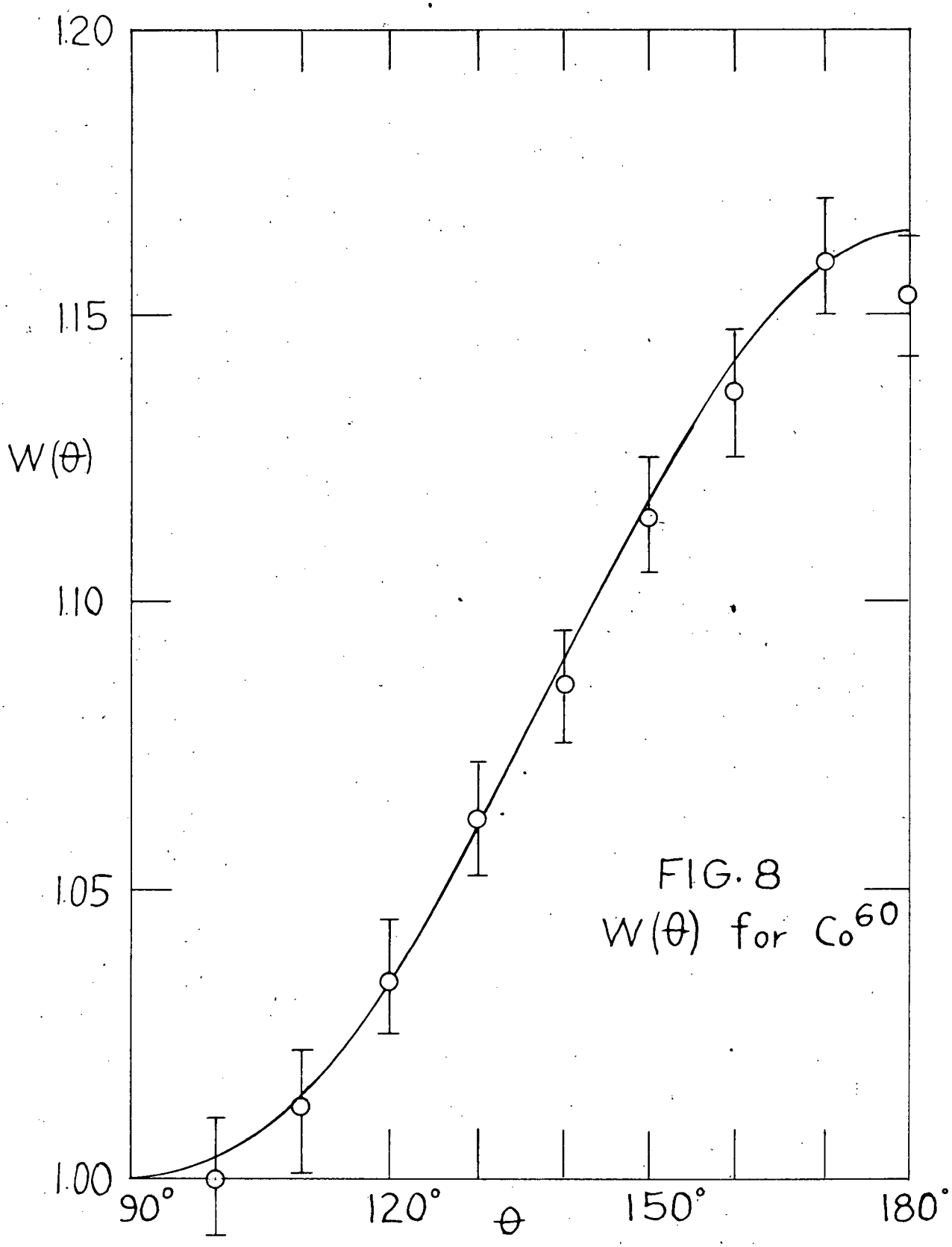

FIG. 8
W(θ) for Co^{60}

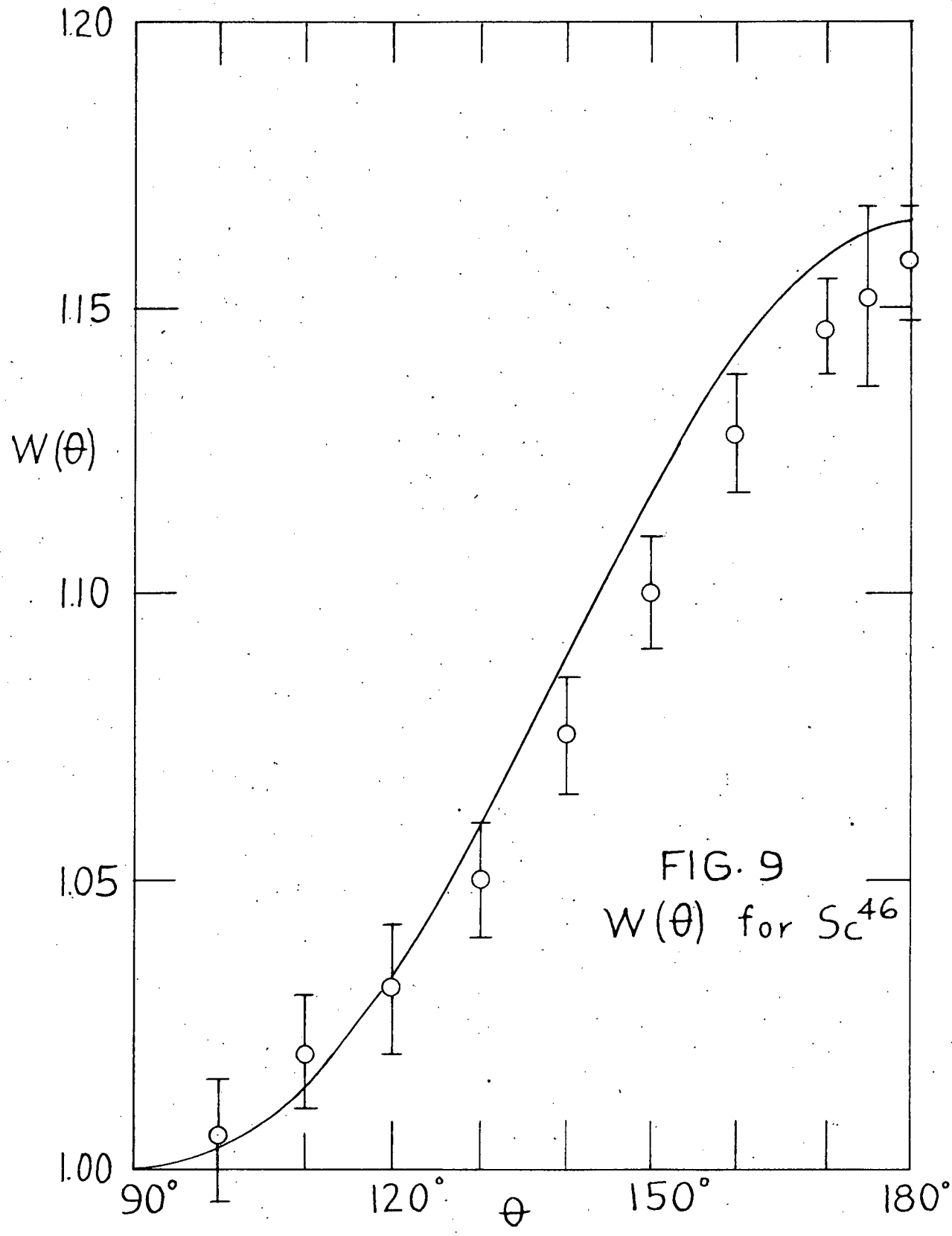

FIG. 9
W(θ) for Sc^{46}

and Sc^{46} respectively. The solid curve in Figs. 8 and 9 represents the function:

$$1 + 0.125 \cos^2\theta + 0.040 \cos^4\theta$$

which is the theoretical function $W(\theta)$ corresponding to the transition $4 \xrightarrow{2} 2 \xrightarrow{2} 0$ as given by Hamilton (2). These results are in good agreement with those of Brady and Deutsch (5).

It is worth noting that there is a small systematic deviation of the experimental curves from the theoretical values in both Co^{60} and Sc^{46}. The correlation is slightly less than predicted in both cases. These deviations are possibly explained by the precession of the nucleus during the lifetime of the intermediate state, which would be expected to reduce the angular correlation, (9). Such a precession might arise due to a magnetic field at the nucleus from an excited electronic state. The product nucleus may be in an excited electronic state for a short time, following the beta decay process. Frauenfelder (22) has performed an experiment on In^{111} in an attempt to show this effect. The results indicate that the effect is likely small if the source is metallic, but may be appreciable for crystalline sources, especially when very thin. The small deviations of the Co^{60} and Sc^{46} correlation curves (Figs. 8 and 9) from the theoretical values are in qualitative agreement with the results of Frauenfelder, since the Co^{60} source was metallic and the Sc^{46} source was in the form of Sc_2O_3. Further investigation of this effect would require considerable refinement of experimental technique.

IV.

THEORY OF BETA-GAMMA ANGULAR CORRELATION

Falkoff and Uhlenbeck (23) have also applied their general theory on angular correlation (15) to the particular case of the beta-gamma angular correlation. In order to apply the results of the first paper to beta-gamma-angular correlations it is only necessary to obtain the angular distributions $F_L^M(\theta)$ for the various possible beta-neutrino interactions. However the interactions involve the beta energy, W, so the angular distributions are $F_L^M(\theta\ W)$, and are called <u>differential</u> angular distributions. If the distributions are integrated over all beta energies, so called <u>integrated</u> angular distributions are obtained:

$$F_L^M(\theta;W_0) = \int_1^{W_0} p\,W(W_0-W)^2\,F_L^M(\theta,W)\,dW .$$

Correspondingly, we have two kinds of beta-gamma angular correlation functions: the <u>differential</u> correlation functions : $W(\theta, E)$ (E is the beta particle K.E.) and $W(\theta, E_0)$ the <u>integrated</u> correlation function. (E_0 is the maximum beta particle K.E.). Falkoff and Uhlenbeck (23) have derived the necessary distribution functions $F_L^M(\theta,W)$ for the five possible beta-neutrino interactions, for the first and second forbidden transitions. It is possible therefore to compute the angular correlation functions from the results of their previous paper (15).

The following results of the theory are useful in the interpretation of angular correlation data:

(See Falkoff and Uhlenbeck (23)).

1. There is no angular correlation for allowed beta transitions.

2. In the case of a forbidden beta transition, the beta spectrum must have a "forbidden shape" for angular correlation to exist.

3. For first forbidden beta-transitions, $W(\theta)$ has the form: $1 + a \cos^2\theta$. For second forbidden beta-transitions a term in $\cos^4\theta$ may occur as well.

4. The differential angular correlation is greatest for beta particles of maximum energy in the beta-spectrum, and is almost isotropic for beta-particles near zero K.E.

5. The above theory assumes that a beta particle leaving the nucleus can be represented by a plane wave, which amounts to assuming that the nuclear charge z is zero. Consequently the theory gives only approximate results. Fuchs and Lennox (24) have made some calculations taking into account the z-dependence, and have shown that for low values of z and certain types of interaction (in particular in the case of the interaction which gives rise to the "Bij-matrix element") the results of the simple theory ($z = 0$) represent a very good approximation.

Since, in general, the form of the integrated beta-gamma angular correlation function is: $W(\theta) = 1 + \sum_i a_i \cos^{2i}\theta$, it is convenient to introduce the integrated angular correlation coefficient, a, defined by:

$$a = \sum_i a_i = \frac{W(180^\circ)}{W(90^\circ)} - 1 .$$

Similarly the differential beta gamma correlation function $W(\theta\ E)$ is of the form: $W(\theta, E) = 1 + \sum_i a_i(E) \cos^{2i}\theta$,

and the <u>differential</u> correlation coefficient a(E) is defined as:

$$a(E) = \sum_i a_i(E) = \frac{W(180°,E)}{W(90°,E)} - 1 .$$

V

APPARATUS FOR MEASURING THE INTEGRATED BETA-GAMMA-ANGULAR CORRELATION

The gamma counter as used in the gamma-gamma correlation experiments is quite suitable for this case also. However, since we wish to measure the beta-gamma coincidence rate it is desirable to have a beta counter with a low efficiency for gamma counting, so the background gamma-gamma coincidence rate will be as small as possible. Accordingly a beta counter consisting of anthracene flakes of a thickness of 30 mg/cm^2 connected to a 5819 photo-multiplier was used.

The source was made as thin as possible in order to prevent scattering of the beta particles in the source. The sources were deposited from solution on a zapon film using insuline to obtain a uniform thickness.* The weight was less than 1 mg/cm^2. The source was then enclosed in a 5 in. diameter plastic vacuum chamber to prevent scattering of the beta particles in the air. The beta counter was placed immediately outside the vacuum chamber in front of an aluminium window of 7 mg/cm^2 to allow the beta particles to enter the anthracene. The general arrangement is shown in Fig. 10.

The absence of severe scattering effects may be inferred from an experiment performed on the beta-gamma-correlation in Sc^{46}. The beta-gamma coincidence rate is isotropic in this case as Novey (14) has reported. With the set up as described in this section, the beta-gamma coincidence rate was found to be the same in the 90° and 180° positions, within the experimen-

* I am indebted to Dr. M. Kirsch and Dr. K. Starke for advice on the preparation of the sources.

tal accuracy of about 1%. It was concluded therefore that the technique did not introduce any serious scattering effects.

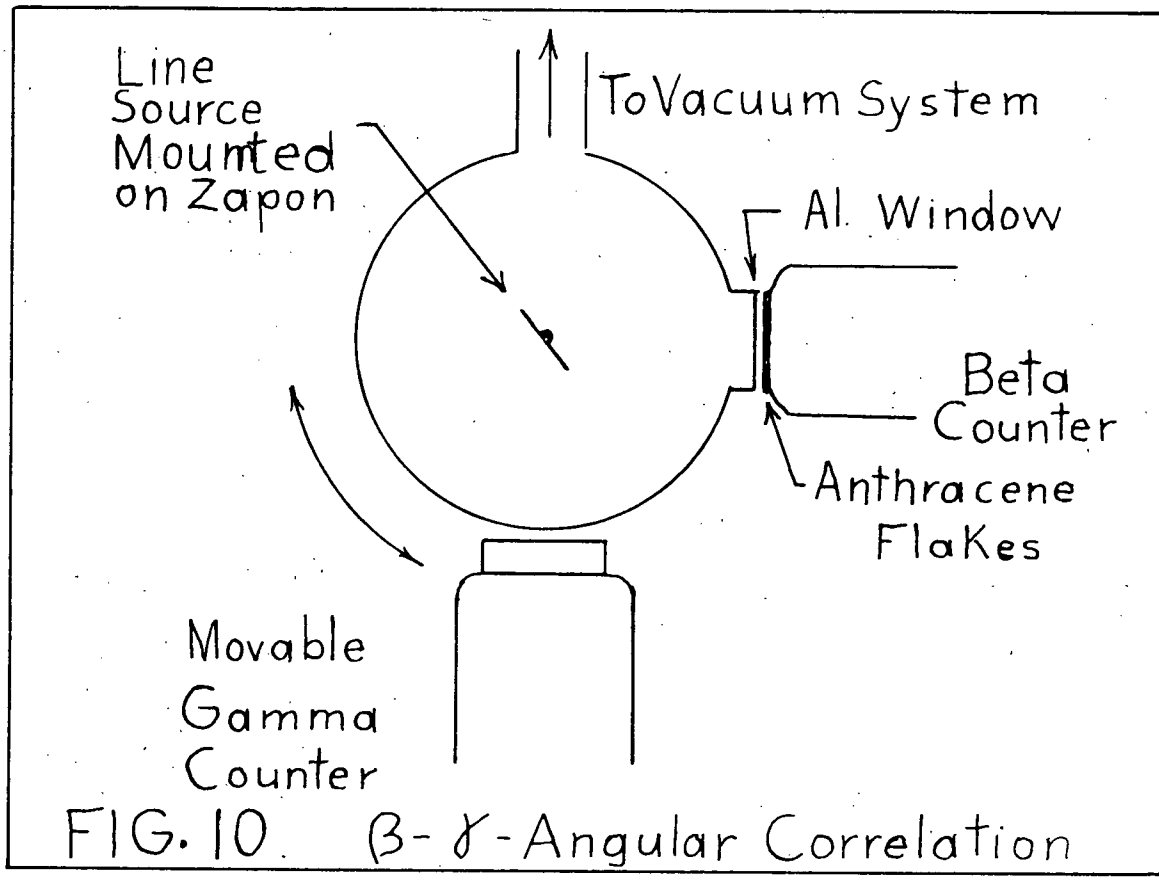

FIG. 10 β-γ-Angular Correlation

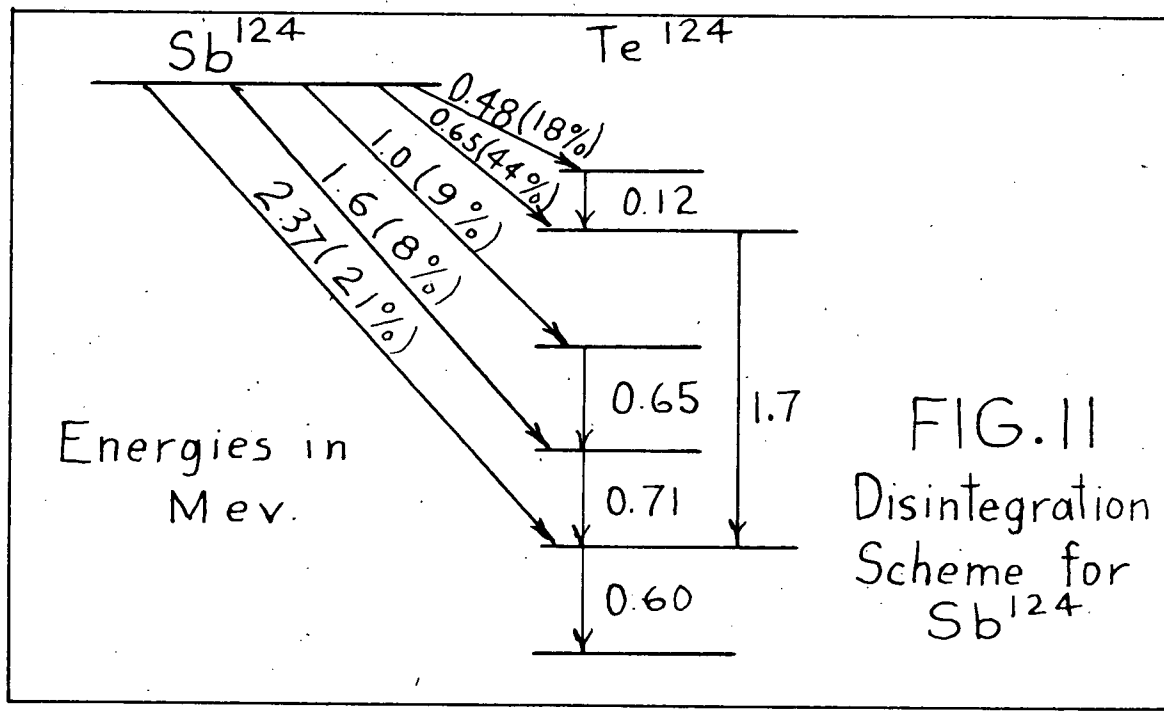

FIG. 11
Disintegration
Scheme for
Sb^{124}

VI

INTEGRATED BETA-GAMMA-ANGULAR CORRELATION IN Sb^{124}.

Many nuclei have been investigated for beta-gamma angular correlation, but in most cases the distribution was found to be isotropic. At the time this research was undertaken only three cases had been reported in which the correlation was not isotropic, namely Sb^{124}, (11) (12) Tm^{170}, (14) and Rb^{86}(13). There appeared to be considerable doubt as to the validity of the results for Tm^{170} and Rb^{86},* while in the case of Sb^{124} the reported results were contradictory, but pointed to the definite existence of an angular correlation effect. Ridgway (11) reported the integrated correlation coefficient for Sb^{124} as $a = -0.17$ while Beyster and Wiedenbeck (12) gave $a = -0.26$. It was hoped that if the integrated angular correlation coefficient had a value $|a| > 0.20$ it would be possible to make a measurement of the differential angular correlation coefficient $a(E)$. An Sb^{124} source was therefore obtained from Chalk River and an experiment performed to obtain the integrated angular correlation coefficient.

The disintegration scheme of Sb^{124} (21) is rather complicated as shown in Fig. 11. The beta-gamma-angular correlation involves the highest energy beta group with 2.37 Mev endpoint and the following 600 Kev gamma ray. If we absorb the beta particle with energy less than about 1 Mev, the beta-gamma coincidence rate

---

*The presence of a beta-gamma-angular correlation in Rb^{86} has since been confirmed by Stevenson and Deutsch (18).

will involve mainly the 2.37 beta group and the 600 Kev gamma ray, with a few coincidences due to the 1.6 Mev beta group. A thin beta counter as described in the preceding section was used. Of course the large number of gamma rays gives a relatively high counting rate in the gamma counter, which contributes to the accidental coincidence rate. The ratio, D, of gamma-gamma to beta-gamma-coincidences was 0.115. The gamma-gamma coincidence rate shows little if any angular correlation in this case, being isotropic within the experimental accuracy of about 5%. The source was prepared by depositing sodium antimonate from solution on to a zapon film using insulin to obtain a uniform thickness. An aluminium beta absorber weighing 270 mg/cm^2 was used in front of the beta counter. This absorber removes all beta particles of less than about 0.9 Mev energy, so we obtain the angular correlation function integrated over all beta energies greater than 0.9 Mev. The value 0.9 Mev was estimated from Feather's energy-range relationship: $R = 0.542E - 0.133$ where R is the range in gms/cm^2 and E is the energy in Mev. The total range of an electron which produced a count was about 310 mg/cm^2.

The function $W(\theta)$ as determined for Sb^{124} is given in Table III and Fig. 12. The evaluation of the data was carried through as developed in Appendices II and VI and consisted of the following consecutive steps:

1. The recorded data consisted of $C(\theta)$, the number of coincidences in time T, the single channel counting rates (scaled by 640), A & B, and D, the ratio of gamma-gamma to beta-gamma coincidence rate. (D was determined by absorbing the beta particles completely in aluminium).

TABLE III

Integrated Angular Correlation in Sb^{124}

θ	$C_T(\theta)$	W(θ)-1	W(θ) -1	W(θ)	S.D.
90°	364	-0.000	-0.000	1.000	0.000
100°	364	-0.000	-0.000	1.000	0.012
110°	358	-0.017	-0.019	0.980	0.008
120°	350	-0.038	-0.043	0.955	0.008
130°	336	-0.077	-0.086	0.910	0.008
140°	320	-0.120	-0.134	0.860	0.008
150°	311	-0.146	-0.163	0.830	0.010
160°	301	-0.173	-0.193	0.799	0.008
170°	296	-0.189	-0.212	0.778	0.011
180°	293	-0.197	-0.220	0.770	0.007

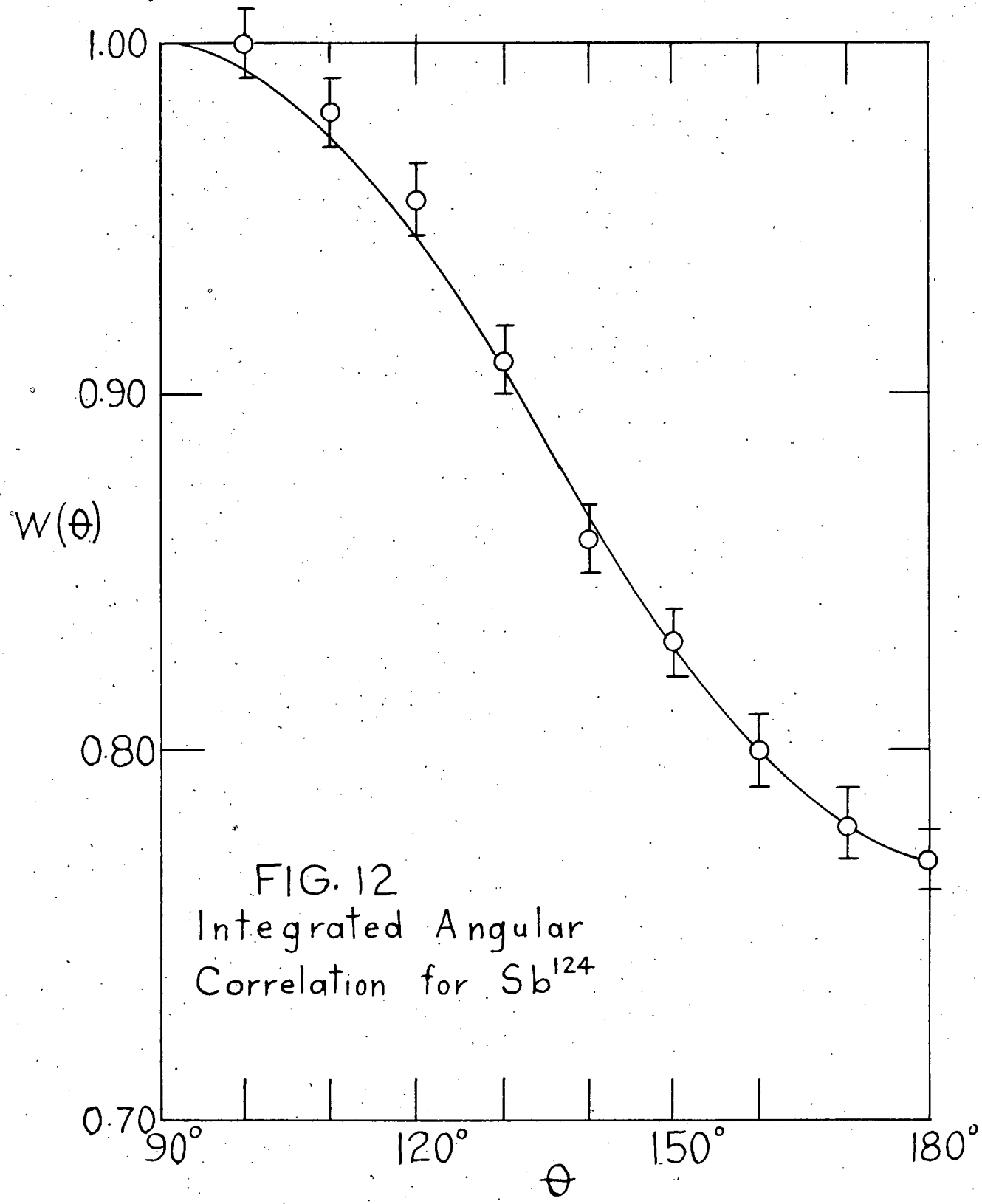

FIG. 12
Integrated Angular
Correlation for Sb^{124}

2. The accidental coincidences were subtracted from $C(\theta)$ and the result divided by the product of the single channel counting rates giving:

$$C_T(\theta) = \left(\frac{C(\theta)\, T}{A\, B} - 2\tau \right).$$

3. The uncorrected correlation function: $\overline{\overline{W}}(\theta) = \frac{C_T(\theta)}{C_T(90^\circ)}$ was computed.

4. The correction for the gamma-gamma background was applied to $\overline{\overline{W}}(\theta)$, thus obtaining: $\overline{W}(\theta) = \overline{\overline{W}}(\theta) \cdot \frac{1}{1-D} - P_\gamma \cdot \frac{D}{1-D}$.

(Appendix VI).

5. The correction for angular resolution was then applied in order to obtain $W(\theta)$, the true correlation function.

The plotted results (Fig. 12) can be fitted closely by a curve (solid line in Fig. 12) of the form: $W(\theta) = 1 + a \cos^2\theta$ where $a = -0.23 \pm 0.01$. Unfortunately it is difficult to compare this result directly with the theory so the discussion will be left until the next section on the differential correlation coefficient in Sb^{124}. It may be remarked however that this result is in fairly good agreement with that of Beyster and Wiedenbeck (12), particularly since the exact range of beta ray energies counted is somewhat uncertain in both cases.

VII

BETA-GAMMA ANGULAR CORRELATION AS A FUNCTION OF ENERGY FOR Sb^{124}.

The theory of the beta-gamma-angular correlation predicts that the effect will increase in magnitude for higher energy beta particles of the spectrum. In the case of Sb^{124} the integrated angular correlation coefficient was found to have a value: $a \simeq -0.23$, only beta particles of energy higher than 0.9 Mev (i.e. up to 2.4 Mev) contributing to this value. The effect should therefore be of such a magnitude near the end of the beta spectrum as to be easily observed, despite the small number of beta particles. An experiment was therefore devised to measure the differential beta-gamma-angular correlation coefficient a(E), defined previously (p. 17).

In order to measure a(E) it is necessary to employ some type of spectrometer as the beta detector. It has been shown by Hopkins (25) that the pulses produced in a thick anthracene crystal scintillation counter by beta particles are proportional to the beta K.E. energy, at least in the energy range 0.1 - 3.0 Mev. It was therefore proposed to use a scintillation spectrometer as the beta detector with a twelve channel kicksorter of Chalk River design as the pulse amplitude discriminator. The apparatus was arranged as shown in Fig. 13 and functions as follows. The kicksorter and scintillation counter circuit is calibrated by determining the endpoint of the Sb^{124} 2.37 Mev beta group pulse spectrum. The twelve kicksorter channels are then adjusted to cover equal energy intervals of about 0.1 Mev over the beta spectrum from 1.0 Mev to 2.37 Kev. Details of this calibration are given in Appendix V. The coincidence mixer

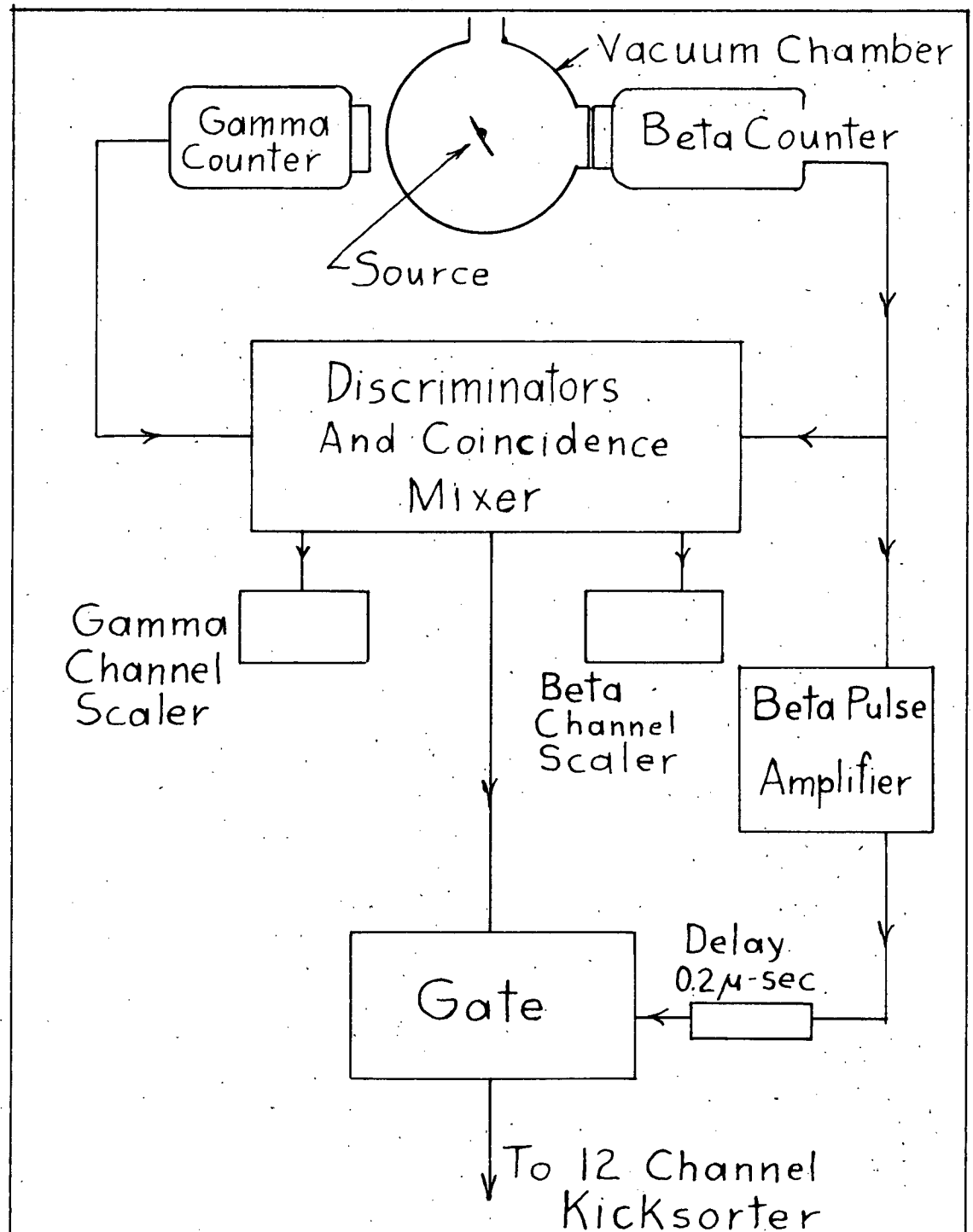

FIG. 13 Differential β-γ-Angular Correlation

has the discriminator in the beta channel set at about 0.9 Mev, so that only those beta-gamma coincidences are detected for which the beta energies are greater than this value. Each coincidence count operates the gate circuit which opens to permit the beta pulse to reach the kicksorter. In this manner the energies of each beta particle which has been counted in coincidence with a gamma ray is recorded. By measuring the coincidence rates at the 90° and 180° positions of the two counters it is possible to determine the angular correlation coefficient as a function of beta energy, that is $a(E)$.

Since the beta counter now employs a thick crystal, it is sensitive to gamma rays as well. The ratio of gamma-gamma to beta-gamma coincidences D may be estimated making reference to Fig. 11. The beta counter is biased to about 1 Mev so only the 1.7 Mev gamma ray which occurs in 60% of the disintegrations, will contribute to the gamma-gamma coincidence rate. The counting efficiency is estimated at about .02 for this gamma ray. The 2.4 Mev beta group comprises 20% of the disintegrations and roughly a half of the beta particles are counted. On the average therefore we would expect to find a value of :

$$D \simeq \frac{0.02 \cdot 0.6}{0.2 \cdot 0.5} = 0.12 .$$

The values measured experimentally for D ranged from 0.15 to 0.20 (see Appendix VI).

Coincidence measurements were taken alternately in the 90° and 180° counter positions for periods of about 12 hours. This procedure tends to average out the effects of small variations in amplifier gain and photo multiplier high tension. The results of five or six days counting in this

fashion were averaged and the differential correlation coefficient a(E) computed. A group of readings such as this will be referred to as a run.

The same computation procedure as was described on page 22 in connection with the integrated correlation coefficient is applied in this case to each kicksorter channel, with two minor changes, as follows:

1. Since the source decays appreciably in six or seven days (half life equals 60 days) a correction must be applied to $C_T(\theta)$ as illustrated in Appendix II.

2. In order to obtain the accidental coincidence rate for each kicksorter channel, first of all, the beta counter pulse spectrum N(E) is obtained on the kicksorter by "opening" the "gate" circuit. Then the total accidental coincidence rate is computed in the usual manner and the accidental rates for each kicksorter channel are computed as the product of the total accidental rate and N(E). (N(E) is expressed as a fraction of the total beta counter counting rate).

The computational procedure used is illustrated for one run, in Appendix VI.

Three other similar runs were made, however the computations are not tabulated here in detail. Fig. 14 gives the values for a(E) for all four runs. The values were combined as shown in Table IV and Fig. 15 to give a single curve. Also plotted in Fig. 15 are two possible theoretical curves (dashed) which will be discussed in the next section.

It is possible to calculate the integrated angular correlation coefficient from the differential correlation

TABLE IV

The Beta-Camma-Angular Correlation Coefficient

a(E) for Sb^{124}

Run	Energy	1.06	1.16	1.26	1.36	1.46	1.56	1.66	1.76	1.86	1.96	2.07	2.17
1	a(E)	0.188	0.208	0.219	0.249	0.273	0.298	0.327	0.368	0.380	0.410	0.414	0.448
	S.D.	0.013	0.015	0.016	0.017	0.018	0.020	0.023	0.026	0.034	0.045	0.053	0.070
2	a(E)	0.211	0.220	0.237	0.272	0.288	0.315	0.328	0.346	0.370	0.388	0.431	0.445
	S.D.	0.014	0.015	0.015	0.017	0.018	0.020	0.023	0.025	0.029	0.033	0.047	0.065
3	a(E)	0.196	0.224	0.254	0.280	0.308	0.334	0.360	0.382	0.400	0.412	-	-
	S.D.	0.019	0.020	0.021	0.021	0.021	0.022	0.025	0.025	0.030	0.030		
4	a(E)	0.188	0.218	0.250	0.280	0.314	0.346	0.380	0.408	0.420	0.436	0.440	0.444
	S.D.	0.016	0.017	0.017	0.017	0.019	0.021	0.024	0.026	0.023	0.028	0.038	0.040
Aver-age	a(E)	0.095	0.218	0.240	0.270	0.296	0.323	0.349	0.376	0.393	0.411	0.428	0.446
	S.D.	0.008	0.009	0.009	0.009	0.010	0.010	0.012	0.013	0.014	0.018	0.026	0.040

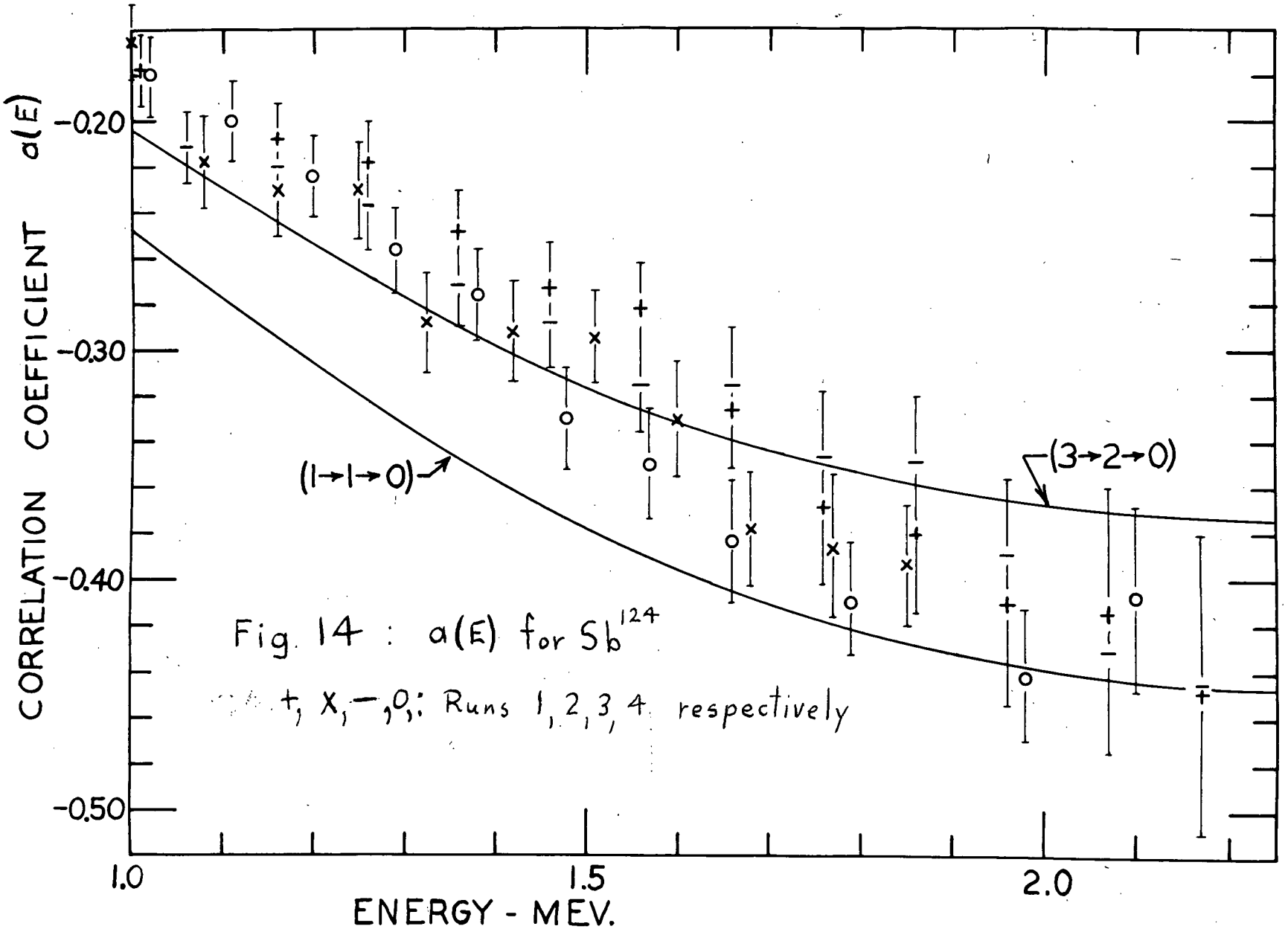

Fig. 14 : a(E) for Sb^{124}

+, X, −, 0; Runs 1, 2, 3, 4 respectively

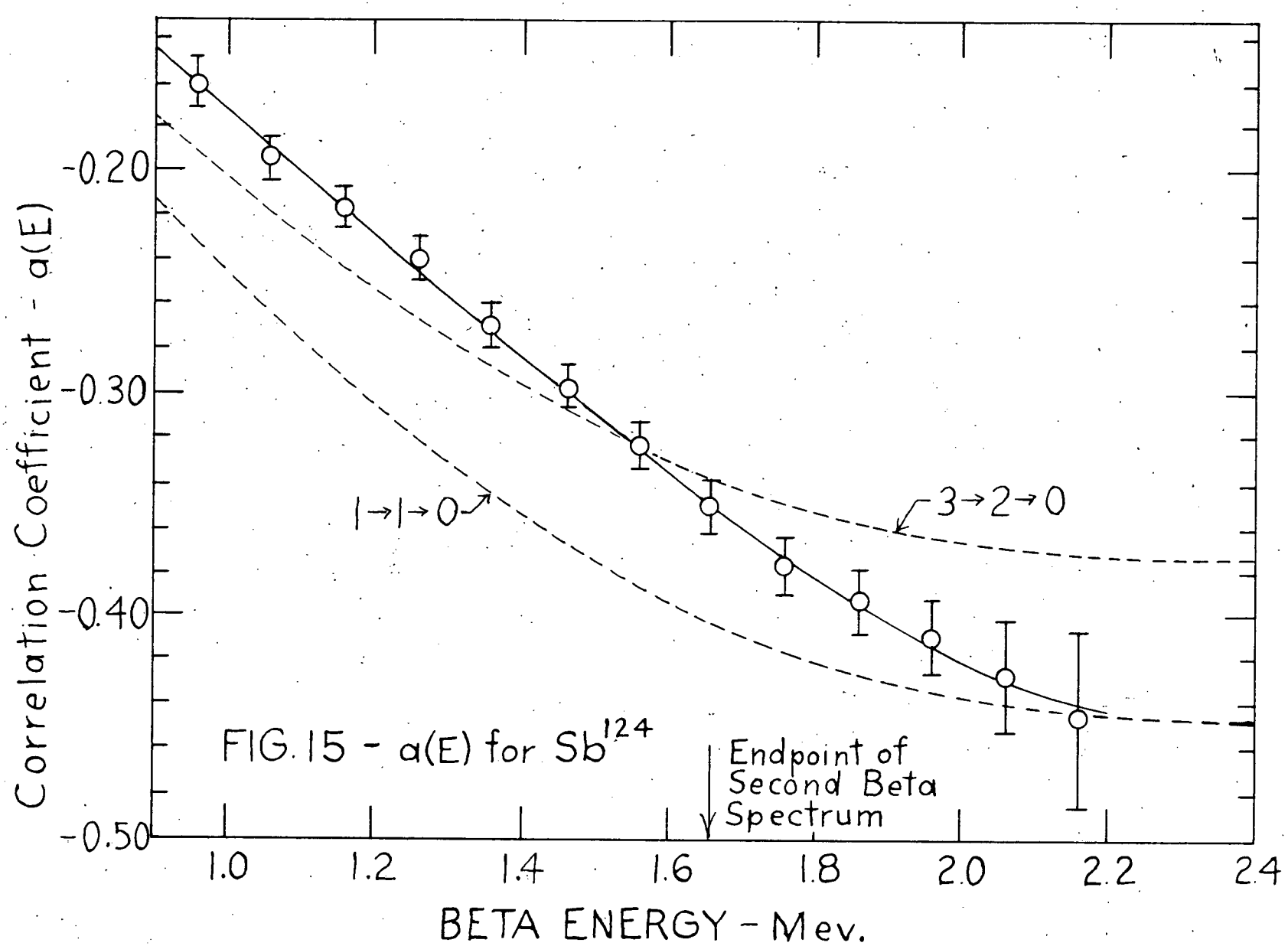

FIG. 15 - a(E) for Sb^{124}

coefficient and the beta spectrum N(E). The details of the method are given in Appendix VIII where it is shown that:

$$a = \frac{\int_{E_c}^{E_o} a(E)\,\frac{N(E)}{a(E)+3}\,dE}{\int_{E_c}^{E_o} \frac{N(E)}{a(E)+3}\,dE},$$

where N(E) is the beta spectrum as measured on the kicksorter. The integration is performed numerically in Table V, for the energy range from $E_c = 0.82$ Mev. to $E_o = 2.37$ Mev. in which we have measured a(E). The value so obtained is $a = -0.24 \pm 0.02$.

The problem of comparing this value with the directly measured integrated correlation coefficient a is complicated by the fact that the true beta spectrum N(E) is distorted by the aluminum absorber used to remove the lower energy beta particles in the case of the direct measurement of a. It is shown in Appendix XI that the value of a which we would expect to measure directly, may be estimated by making some assumption for the amount of distortion of N(E) and integrating a(E) in a manner similar to Table V. The result of this estimate is that a should lie between the values $a = -0.24 \pm 0.02$ to -0.27 ± 0.02, depending on the amount of absorption of N(E). The deviation of this estimate from the measured value, $a = -0.23 \pm 0.01$ is about ± 0.02 to ± 0.03. This small deviation may be interpreted as the limit of the systematic error. This systematic error is due to small drifts in amplifier gain and counter high tension. The influence of these drifts on the determination of a(E) is illustrated in Fig. 14, where the results of four separate determinations of a(E) are given.

To conclude, it should be emphasized that it is the value of a as obtained in Table V, i.e. $a = -0.24 \pm 0.02$, which has an unambiguous theoretical meaning.

TABLE V

Integration of $\underline{a(E)}$ to obtain $\underline{a}$

Beta Energy	a(E)	Spectrum N(E)	$\frac{N(E)}{3 + a(E)}$	$\frac{a(E)\ N(E)}{3 + a(E)}$
0.86 Mev	-0.130	25000	8700	-1130
0.96	-0.160	23000	8100	-1296
1.06	-0.190	21000	7470	-1419
1.16	-0.218	19200	6900	-1504
1.26	-0.240	18000	6520	-1564
1.36	-0.270	14970	5480	-1480
1.46	-0.296	13100	4840	-1433
1.56	-0.323	10980	4100	-1324
1.66	-0.349	7690	2900	-1012
1.76	-0.376	6550	2500	-940
1.86	-0.393	5070	1940	-762
1.96	-0.411	3189	1230	-506
2.06	-0.428	1751	681	-291
2.16	-0.446	849	323	-148
		Totals:	61684	-14769

$$a = \frac{-14769}{61684} = -0.24$$

VIII

RESULTS AND CONCLUSIONS REGARDING THE DIFFERENTIAL BETA-GAMMA-ANGULAR CORRELATION FOR Sb^{124}

From Fig. 15 the value of $a(E)$ near the end of the 2.37 Mev beta-spectrum is seen to approach a value in the neighbourhood of $a(E_o) = -0.44 \pm 0.05$. In order to compare this result with theory the following additional information is available. According to Langer et al (26) the 2.37 Mev beta spectrum is very likely of the "alpha-type", corresponding to the first forbidden matrix element B_{ij}. This implies a change of parity and the following possible changes of the angular momentum quantum number: $\Delta j = 0, \pm 1, \pm 2$. Moreover, the product nucleus Te^{124} has a spin in the ground state of 0 since it is an even-even nucleus. If the matrix element B_{ij} is dominant, then the beta particle carries away angular momentum $L_1 = 2$. From these considerations we get for electric dipole gamma radiation, that is $L_2 = 1$, the following possible spin changes:

$$1 \longrightarrow 1 \longrightarrow 0$$
$$2 \longrightarrow 1 \longrightarrow 0$$
$$3 \longrightarrow 1 \longrightarrow 0$$

and for electric quadrupole radiation ($L_2 = 2$)

$$0 \longrightarrow 2 \longrightarrow 0$$
$$1 \longrightarrow 2 \longrightarrow 0$$
$$2 \longrightarrow 2 \longrightarrow 0$$
$$3 \longrightarrow 2 \longrightarrow 0$$
$$4 \longrightarrow 2 \longrightarrow 0$$

The tables and formulae given by Falkoff and Uhlenbeck (23) have been used to calculate the value of the correlation coefficient for the maximum beta energy Eo = 2.37 Mev for each of the above cases. Further details of the procedure involved are given in Appendix IX. The values for $a(E_o)$ so obtained are listed, Table VI. The values of $a(E_o)$ for the transition schemes $1 \longrightarrow 1 \longrightarrow 0$, $3 \longrightarrow 2 \longrightarrow 0$ are relatively close to the experimental value, so the complete functions a(E) were evaluated in these two cases. The curves so obtained are shown in Fig. 15.

In interpreting these results, it must be remembered that in the energy range 1.0 Mev - 1.6 Mev two beta groups are superimposed. The 1.6 Mev group presumably has no beta-gamma-angular correlation, since the magnitude of the correlation coefficient decreases rapidly below 1.6 Mev. With this in mind the results favour the transition scheme $1 \longrightarrow 1 \longrightarrow 0$ since any error would presumably tend to make the correlation more isotropic. There is, however, a serious difficulty in accepting this assignment, because the beta transition directly to the Te^{124} ground state would then be allowed, or at the most, first forbidden. It is then difficult to account for the scarcity of these transitions.

Very recently Nakamura et al (27) have attempted to provide an alternative interpretation of the results of Langer et al (26). Nakamura has considered ft values and the nuclear shell model in his interpretation, but has given no consideration to angular correlation data at all. His theoretical conclusions seem to be incompatible with our experimental results. However, further consideration is being given to the problem in an attempt

TABLE VI

Transition	$a(E_o)$
$1 \longrightarrow 1 \longrightarrow 0$	-0.44
$2 \longrightarrow 1 \longrightarrow 0$	+0.64
$3 \longrightarrow 1 \longrightarrow 0$	-0.14
$0 \longrightarrow 2 \longrightarrow 0$	+0.73
$1 \longrightarrow 2 \longrightarrow 0$	+0.86
$2 \longrightarrow 2 \longrightarrow 0$	-0.15
$3 \longrightarrow 2 \longrightarrow 0$	-0.37
$4 \longrightarrow 2 \longrightarrow 0$	+0.23
Experimental Value:	-0.44 ± 0.04

to obtain a satisfactory theoretical interpretation of all experimental data which is now available concerning Sb^{124}.

A few months after the publication of our preliminary report (16), Stevenson and Deutsch (18) have published the results of their measurement of the differential beta-gamma angular correlation a(E) for Sb^{124} in which they made use of a magnetic beta ray lens spectrometer. There is excellent agreement between their results and ours, though the two methods are quite different.

It is worthwhile noting the present state of beta-gamma-angular correlation experimentation. Angular correlation effects have been reported and the integrated beta-gamma-angular correlation coefficient measured for the following nuclei: Sb^{124} (12), Rb^{86} (13), I^{126} (18), Tm^{170} (11) and K^{42} (28). Only for Sb^{124}(17)(18) and Rb^{86}(18) has the differential angular-correlation-coefficient been reported. No angular correlation has been found for most commonly obtainable radioactive nuclei, including: Co^{60}, Na^{22}, Na^{24}, Co^{134}, Sc^{46}, and I^{124}.

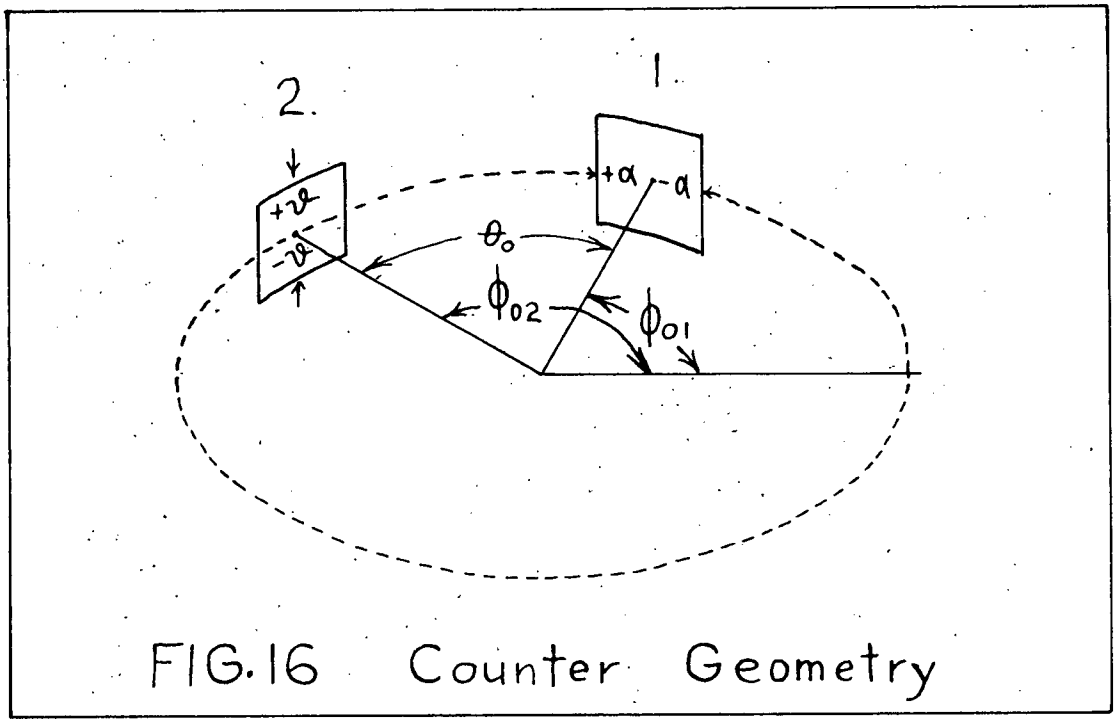

FIG. 16 Counter Geometry

APPENDIX I.

COINCIDENCE COUNTING WITH DIRECTIONAL CORRELATION BETWEEN THE EMITTED PARTICLES.

A simple cascade disintegration scheme is illustrated in Fig. 1 B. Let us assume that counter 1 counts only the first particle emitted, and the second counter counts only the second particle. Let us denote the probability of the counter 1 for detecting particle 1 whose direction falls within an infinitesimal solid angle $d\omega_1$ around a direction characterized by the unit vector $\vec{\omega}_1$ as: $\vec{e}_1(\vec{\omega}_1)\,\frac{d\omega_1}{4\pi}$. Then the single counting rate in counter 1 is $N_1 = N_0 \epsilon_1$, where N_0 is the source strength (disintegrations per sec.) and

$$\epsilon_1 = \frac{1}{4\pi}\int \vec{e}_1(\vec{\omega}_1)\, d\omega_1 ,$$

the integration being over the whole sensitive area of the counter. Introducing a similar notation for counter 2, we get, referring to Fig. 16, for the differential coincidence counting rate:

$$N_c(\theta) = N_0 \frac{\vec{e}_1(\vec{\omega}_1)d\omega_1}{4\pi} \cdot \frac{\vec{e}_2(\vec{\omega}_2)d\omega_2}{4\pi} \cdot W(\vec{\omega}_1, \vec{\omega}_2)$$

where $W(\omega_1, \omega_2) = W(\theta)$ is the angular correlation function, θ being defined by: $\cos\theta = \frac{\vec{\omega}_1 \cdot \vec{\omega}_2}{\omega_1 \omega_2}$. If we integrate between the limits indicated in Fig. 16, making the assumption that the counters 1 and 2 both subtend the same angles at the source we obtain the total coincidence rate:

$$\bar{N}_c = \frac{N_0}{(4\pi)^2}\left[\int_{\varphi_{01}-\alpha}^{\varphi_{01}+\alpha} d\varphi_1 \int_{-\vartheta}^{+\vartheta} d\vartheta_1 \cos\vartheta_1\, \vec{e}_1(\varphi_1,\vartheta_1) \int_{\varphi_{02}-\alpha}^{\varphi_{02}+\alpha} d\varphi_2 \int d\vartheta_2 \cos\vartheta_2\, \vec{e}_2(\varphi_2,\vartheta_2)\cdot W(\varphi_1,\vartheta_1,\varphi_2,\vartheta_2)\right]$$

The subscripts 1 and 2 refer to counters 1 and 2, while 01,02 refer to the center position of counters 1 and 2 respectively. If we assume $\vec{e}_1$ and $\vec{e}_2$ are constant over directions $\vec{\omega}_1$ and $\vec{\omega}_2$, and introduce the variables: $\alpha_1 = \varphi_1 - \varphi_{01}$ and $\alpha_2 = \varphi_2 - \varphi_{02}$, we obtain from the previous expression for $\overline{N}_c$:

$$\overline{N}_c = \frac{N_0 e_1 e_2}{(4\pi)^2}\left[\int_{-\vartheta}^{+\vartheta} d\vartheta_1 \cos\vartheta_1 \int_{-\vartheta}^{+\vartheta} d\vartheta_2 \cos\vartheta_2 \int_{-\alpha}^{+\alpha} d\alpha_1 \int_{-\alpha}^{+\alpha} d\alpha_2\, W(\varphi_{01}+\alpha_1, \vartheta_1; \varphi_{02}+\alpha_2, \vartheta_2)\right].$$

From the fact ϑ is small (10°) we now introduce the approximations that $\cos\vartheta \simeq 1$ and ϑ can be neglected in comparison with θ, that is: $\theta = \theta_0 + \alpha_2 - \alpha_1$.

If we assume that $W(\theta)$ has the simplest form consistent with the theory:

$$W(\theta) = W(\theta_0 + \alpha_2 - \alpha_1) = 1 + a\cos^2(\theta_0 + \alpha_2 - \alpha_1),$$

elementary integration gives us:

$$\overline{N}_c(\theta_0) = N_0 \epsilon_1 \epsilon_2 \left[1 + a\left(\frac{1}{2} - \frac{1}{2}\frac{\sin^2 2\alpha}{(2\alpha)^2} + \frac{\sin^2 2\alpha}{(2\alpha)^2}\cos^2\theta_0\right)\right],$$

Where $\epsilon_1 = \frac{e_1 \cdot (2\alpha)(2\vartheta)}{4\pi}$ and $\epsilon_2 = \frac{e_2 (2\alpha)(2\vartheta)}{4\pi}$.

As α, ϑ become very small we obtain ideal resolution, for which case the coincidence rate $N_c(\theta_0)$ is:

$$N_c(\theta_0) = N_0 \epsilon_1' \epsilon_2' \left(1 + a\cos^2\theta_0\right).$$

We have assumed that counter 1 has an efficiency of zero for the detection of the second particle, and similarly that counter 2 has zero efficiency for the detection of the first particle emitted. This condition can be obtained, practically, for beta-gamma coincidences. However if these efficiencies

are not zero, the coincidence rate as expressed in the previous formulae must include a second term, similar to the first one, but involving these efficiencies. The case in which both gamma rays are of about the same energy (nearly realized for Co^{60}) is particularly simple, since the coincidence rates are then given by the preceding formula with an additional factor of two.

APPENDIX II.

PROCEDURE TO EVALUATE THE TRUE COINCIDENCE RATE.

The angular resolution of the counters was chosen so that $2\alpha = 2\vartheta = 20^\circ = 0.349$ radians (Fig. 16). If we assume that $W(\theta) = 1 + a\cos^2\theta$, which is the simplest form consistent with the theory, the coincidence counting rate for ideal resolution is:

$$N_c(\theta) = N_0 \epsilon_1 \epsilon_2 \left[1 + a\cos^2\theta\right].$$ (See Appendix I).

Upon substitution of the above numerical values for the subtended counter angles we obtain for the observed coincidence rate:

$$\bar{N}_c(\theta) = N_0 \epsilon_1' \epsilon_2' \left[1 + a(0.021 + 0.958\cos^2\theta)\right].$$

We have assumed that:

$$W(\theta) - 1 = a\cos^2\theta = \frac{N_c(\theta) - N_c(90^\circ)}{N_c(90^\circ)}.$$

Let us now define the experimentally observed angular correlation function as follows:

$$\bar{W}(\theta) - 1 = \frac{\bar{N}_c(\theta) - \bar{N}_c(90^\circ)}{\bar{N}_c(90^\circ)},$$ and determine the correction required in order to obtain $W(\theta)$ from it. Applying the formula for $\bar{N}_c(\theta)$, we obtain:

$$\bar{W}(\theta) - 1 = \frac{0.958\, a\cos^2\theta}{1 + 0.021\, a},$$

and since a is generally small (about 0.2) this may be written:

$$\bar{W}(\theta) - 1 \simeq 0.958 a\cos^2\theta - 0.020\, a^2\cos^2\theta.$$

We therefore obtain the proper correction to be applied to $\bar{W}(\theta)$

to obtain $W(\theta)$ as follows:

$$W(\theta) = \overline{W}(\theta) + 0.042\, a \cos^2\theta + 0.020\, a^2 \cos^2\theta .$$

A possible procedure is to plot $\overline{W}(\theta) - 1$ and obtain an approximate value for a which may be used with sufficient accuracy in the correction formula above to obtain $W(\theta)$.

In actual practice the observed coincidence rate, N_{OBS}, is partly due to accidental coincidences. This accidental coincidence rate, N_A, may be calculated from the individual counter rates N_1, N_2, as follows:

$N_A = 2\tau N_1 N_2 = 2\tau N_0^2 \epsilon_1 \epsilon_2$, τ being the mixer resolving time (0.18 μ-sec.). Consequently N_{OBS} is given by:

$$N_{OBS} = \overline{N}_c(\theta) + N_A = N_0 \epsilon_1 \epsilon_2 \overline{W}(\theta) + 2\tau N_0^2 \epsilon_1 \epsilon_2 .$$

Now N_{OBS} may vary slightly due to fluctuations in H.T. supply and amplifier gain, but this may be corrected for by dividing by $(N_1 \times N_2)$ since this gives us a quantity which is independent of the counter efficiencies as follows:

$$\frac{N_{OBS}}{N_1 \cdot N_2} = \frac{\overline{W}(\theta)}{N_0} + 2\tau .$$

If C is the total number of coincidence counts and T is the total time, and letting $A = N_1 T$, and $B = N_2 T$, be the total single channel counts in time T, then from the last two equations it follows that:

$$\frac{N_{OBS}}{N_1 N_2} = \frac{CT}{AB} .$$

For convenience of computation we define a quantity $C_T(\theta)$ as follows:

$$C_T(\theta) \equiv \frac{CT}{AB} - 2\tau = \frac{\bar{w}(\theta)}{N_o} .$$

If the source decays appreciably during the experiment, it will be necessary to apply a correction for this as well. Since, $C_T(\theta) = \frac{\bar{w}(\theta)}{N_o}$ it will increase as the source decays, so the correction consists of multiplying $C_T(\theta)$ by the proper decay factor, f.

APPENDIX III.

COMPTON SCATTERING OF GAMMA RAYS BETWEEN COINCIDENT COUNTERS.

The operation of a scintillation counter as a gamma detector depends upon the gamma ray interacting with the crystal in such a manner as to transfer part, or all of its energy to one or more electrons. Pair production, photo electric effect and Compton scattering are possible methods for such an interaction to take place. For gamma rays with energy of the order of 1 Mev, Compton scattering is the most probable interaction process. The electron of course produces a scintillation in the crystal which is detected by means of a photo-multiplier.

The scattered photon from the Compton process has a lower energy than the incident photon, but may easily escape from the crystal, and may in fact be scattered in the direction of the other gamma counter. When scattered through 180° the gamma photon has an energy of about 200 Kev (initial energy 1 Mev), so these scattered quanta may easily give rise to a spurious count. In fact the efficiency of the counter may be more than twice as great for the scattered photons than for the incident photons due to the higher total cross section of the crystal for lower energy photons.

The magnitude of this "scattered coincidence rate", $C_s(\theta)$ may be estimated as follows:

$C_s(\theta) = 2\, N_s(\theta)\, \omega' \Delta'$, where $N_s(\theta)$ is the number of photons scattered through an angle θ per unit solid angle per second, Δ' is the counter efficiency for the scattered photon, and ω' is the solid angle subtended between the counters. The factor 2 occurs if we assume that the gamma counters are identical, and that the gamma rays in cascade have nearly the same energy.

$N_s(\theta)$ is given by:

$$\frac{N_s(\theta)}{N_1} = \frac{d\phi}{\phi}$$

where $d\phi$ is the differential Compton cross-section, ϕ is the total Compton cross-section and N_1 is the single channel counting rate. The true coincidence rate, C_T, is given by:

$C_T = 2 N_0 \epsilon_1 \epsilon_2 = N_1 \epsilon_2$, so that we obtain for the ratio of scattered to true coincidences:

$$\frac{C_s}{C_T} = 2 \frac{d\phi}{\phi} \frac{\omega' \Delta'}{\epsilon_2} = 8\pi \frac{d\phi}{\phi} \frac{\omega' \Delta'}{\omega \Delta}$$

where Δ is the efficiency of the gamma counter for the incident photons and ω is the solid angle subtended by the counter at the source.

Assume that the counters and source are arranged symmetrically in a straight line, so that $\omega = 4\omega'$. For a 1 Mev incident gamma ray the scattered gamma (180°) has an energy of 200 Kev. The Compton cross section of the crystals for 200 Kev gammas is about twice that for 1 Mev gamma rays. Therefore if the discriminator is set low enough to count the smaller 200 Kev pulses, the efficiencies are in the ratio $\frac{\Delta'}{\Delta}$ 2.

$\frac{d\phi}{\phi}$ may be determined from the formula and tables in Heitler, Quantum Theory of Radiation, the value for 1 Mev gamma scattered through 180° being $d\phi/\phi = 0.04$. Using these values we obtain $\frac{C_{scatt}}{C_{true}} = 4\pi\ 0.04 \simeq 0.5$. This result gives an order of magnitude only, since the photo electric cross section has been negleeted, however effects of this magnitude have been observed.

APPENDIX IV.

THE STANDARD DEVIATION IN W(Θ).

Experimentally we calculate W(Θ) from the formula:

$$W(\Theta) = \frac{C_T(\theta)}{C_T(90°)} \quad \text{(see Appendix II).}$$

The relative standard deviation is accordingly given by:

$$\left(\frac{\Delta W(\theta)}{W(\theta)}\right)^2 = \left(\frac{\Delta C_T(\theta)}{C_T\theta}\right)^2 + \left(\frac{\Delta C_T(90°)}{C_T(90°)}\right)^2 .$$

The relative error in $C_T(\Theta)$ may be evaluated from the total number of counts obtained, by the means of the well known Poisson Formula. In this case the total count obtained, C, is partly due to accidental coincidences, C_A, so that: $C_T \sim C-C_A$, and accordingly:

$$\left(\frac{\Delta C_T}{C_T}\right) = \frac{\sqrt{C + C_A}}{C - C_A} .$$

APPENDIX V.

CALIBRATION OF THE KICKSORTER CHANNELS IN TERMS OF BETA ENERGY.

According to Hopkins (25) who used a beta counter of similar construction to the one used here, the pulses produced are proportional to the beta energy, at least in the range 0.1 - 3.0 Mev. In order to calibrate the kicksorter it is only necessary to establish one point in the energy spectrum, the endpoint of the 2.37 Mev beta group being the most practical to use. Accordingly, before each run, the beta pulse spectrum was obtained on the kicksorter. It is then necessary to estimate the endpoint of the spectrum and construct a Fermi plot. If the endpoint was selected correctly, a straight line Fermi plot resulted as in Fig. 17. The Fermi plot was concave upwards or downwards depending on whether the original estimate of the endpoint was too high or two low. In this manner the endpoint could be determined to within $\frac{1}{2}$ channel width or $\pm$ 50 Kev. Referring again to Fig. 17, the Fermi plot is seen to be practically a straight line in the range 1.7 to 2.37 Mev, with a sharp break at about 1.65 Mev. This is the endpoint of the second beta group (see Fig. 11) in Sb^{124} and its presence in the Fermi plot lends considerable confidence to the calibration. The calculation of the Fermi plot (Table VII) includes the correction for the forbidden shape of the spectrum, although this is hardly necessary considering the accuracy of the endpoint determination.

TABLE VII

Fermi Plot of Sb^{124} Spectrum

V	ϵ'	$f(52,\eta)\frac{\epsilon}{\eta}$	$N(\epsilon')$	$\frac{N}{f\cdot\epsilon/\eta}$	$\sqrt{\frac{N}{f\cdot\epsilon/\eta}}$	C	$\frac{1}{C}\sqrt{\frac{N}{f\,\epsilon/\eta}}$
625	2.467	28.0	17996	64.27	8.02	3.97	20.2
675	2.664	31.0	14973	48.30	6.95	4.04	17.2
725	2.861	34.2	14048	41.08	6.47	4.13	15.7
775	3.059	37.5	10982	29.29	5.41	4.24	12.8
825	3.256	42.0	7694	18.32	4.28	4.36	9.8
875	3.454	45.5	6555	14.41	3.80	4.50	8.4
925	3.651	49.0	5067	10.34	3.22	4.65	6.9
975	3.842	52.0	3189	6.13	2.48	4.80	5.2
1025	4.046	55.5	1751	3.15	1.78	4.98	3.6
1075	4.243	59.8	849	1.42	1.19	5.17	2.3
1125	4.441	65.0	297	0.46	0.68	5.34	1.3
1175	4.638	67.5	0	0.00	0.00		0:0

V = Kicksorter Channel Bias.

ϵ' = Beta Kinetic Energy in units of mc^2.

$f(52,\eta)$ = The Fermi function for z = 52.

$N(\epsilon')$ = Beta Spectrum.

ϵ = Total beta energy in units mc^2.

η = Beta Momentum in units mc.

$C = \sqrt{(\epsilon_0-\epsilon)^2+\eta^2}$ is the " α -type" forbidden shape factor.

$\epsilon^2 = \eta^2 + 1$.

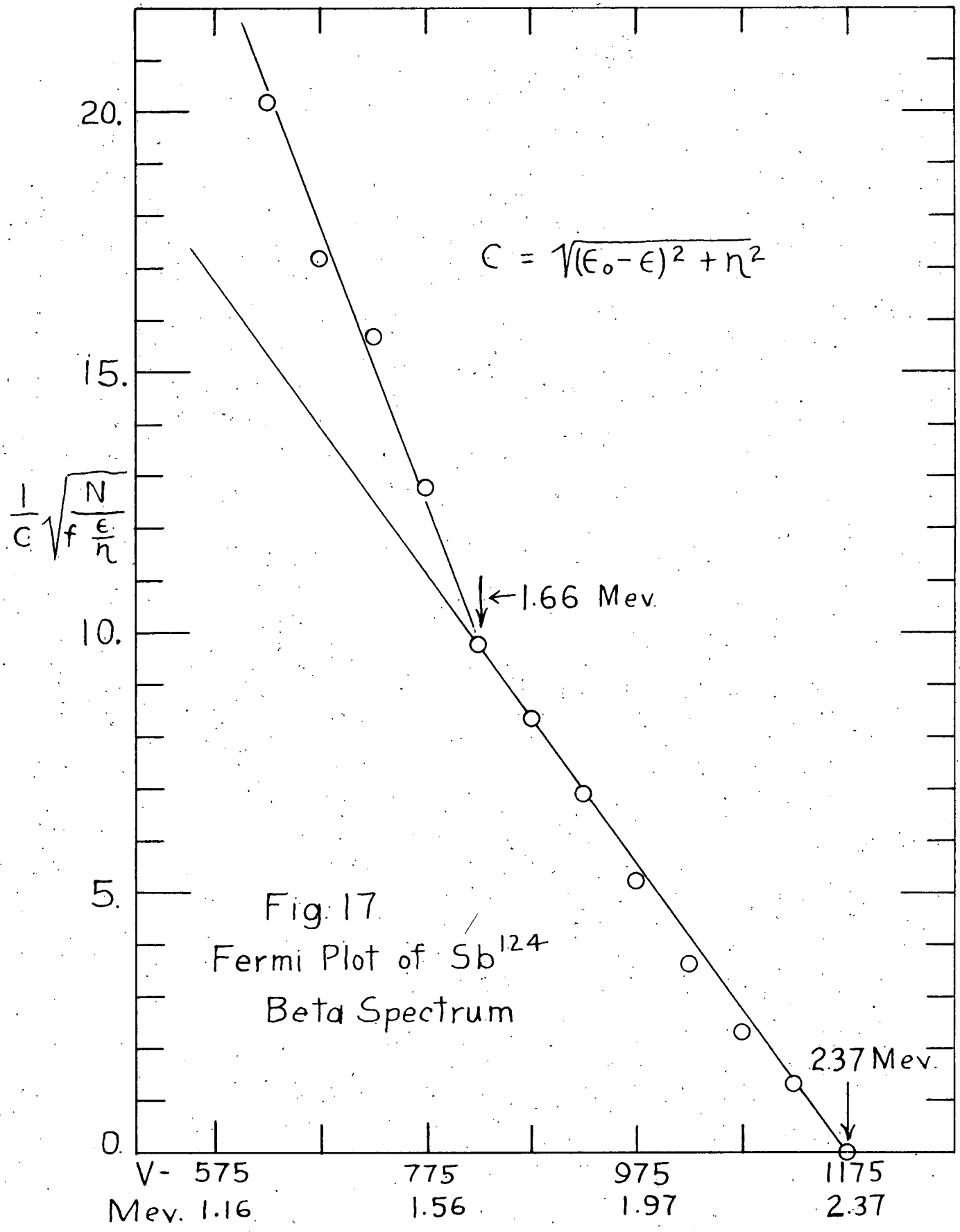

Fig. 17
Fermi Plot of Sb^{124}
Beta Spectrum

APPENDIX VI.

CALCULATION OF BETA-GAMMA ANGULAR CORRELATION COEFFICIENT

If we now consider C to be the total number of coincidence counts in time T we have:

$C = C_{\beta\gamma} + C_{\gamma\gamma} + C_A$, where the subscripts refer respectively to beta-gamma, gamma-gamma, and accidental coincidences respectively. Retaining our definition of Appendix II:

$C_T(\theta) = \frac{CT}{AB} - 2\tau$ and introducing $C_{T\gamma} = \frac{C_{\gamma\gamma} \cdot T}{AB}$,

we have:

$$\bar{a} = \frac{\left[C_T(\pi) - C_{T\gamma}(\pi)\right] - \left[C_T\left(\frac{\pi}{2}\right) - C_{T\gamma}\left(\frac{\pi}{2}\right)\right]}{\left[C_T\left(\frac{\pi}{2}\right) - C_{T\gamma}\left(\frac{\pi}{2}\right)\right]} .$$

The gamma-gamma coincidence background rate is about 15 - 20% of the β-γ coincidence rate.

Let $C_{T\gamma}\left(\frac{\pi}{2}\right) = D \cdot C_T\left(\frac{\pi}{2}\right)$, then:

$$\bar{a} = \frac{C_T(\pi) - C_T\left(\frac{\pi}{2}\right)}{C_T\left(\frac{\pi}{2}\right)(1-D)} - \frac{C_{T\gamma}(\pi) - C_{T\gamma}\left(\frac{\pi}{2}\right)}{C_{T\gamma}\left(\frac{\pi}{2}\right)} \cdot \frac{D}{1-D}$$

$$= \bar{\bar{a}} \cdot \frac{1}{1-D} - P_\gamma \cdot \frac{D}{1-D},$$

where $\bar{\bar{a}}$ is the measured correlation coefficient and P_γ is the gamma-gamma correlation coefficient. $C_{\gamma\gamma}(\theta)$ is measured separately by absorbing the beta particles with aluminium, which gives us P_γ. The correlation for angular resolution may now be applied in the way described in Appendix II.

This procedure is also applied to the data for each kicksorter channel when measuring the differential correlation

coefficient, $a(E)$.

As an example of the procedure followed, Table VIII gives the experimental data for one run in the determination of $a(E)$ for Sb^{124}. The notation used in Table VIII is consistent with the notation used in the formulae in this Appendix. The "Bias" is in arbitrary units and the "Energy" refers to the energy in Mev. corresponding to the kicksorter channel midpoint bias. The "Spectrum" is the pulse spectrum obtained from the beta counter, while the "gamma-spectrum" is the pulse spectrum obtained from the beta counter when the beta particles were absorbed in aluminium. The kicksorter channel rates are in each case expressed as a fraction of the total counting rate obtained from the beta counter for that particular spectrum measurement. The standard deviation "S.D." refers to the statistical error in $a(E)$.

Following the procedure in Appendix II, $C_T(\theta)$ is calculated and multiplied by the appropriate decay factor, F. The recorded data consisted of the time T, the total coincidence counts C in each channel, and the total single channel counts scaled by 640, A and B. $C_T(\theta)$ as given in Table VIII is in these units multiplied by 10^7. Twice the resolving time, 2τ, in this system of units is 407 (hrs x 640^{-2} x 10^{-7}) which is : 407 x 3600 x 640^{-2} x 10^{-7} = 0.356 x 10^{-6} sec. Similarly, for convenience the table records $\frac{T}{AB}$ in units of (hr. x 640^{-2} x 10^{-11}). The total number of true coincidence counts recorded in time T is therefore:

$$C_T(\theta) \cdot \frac{AB}{T} \times 10^4 .$$

TABLE VIII $a(E)$ for Sb^{124}

	Time hrs.	Total	$\frac{I}{AB}$	5.0	5.5	6.0	6.5	7.0	7.5	8.0	8.5	9.0	9.5	10.5	11.5
Bias															
Energy (Mev)				0.94	1.02	1.11	1.20	1.29	1.38	1.48	1.57	1.66	1.79	1.97	2.14
Spectrum.		1.0		0.124	0.110	0.107	0.087	0.081	0.075	0.064	0.053	0.039	0.059	0.028	0.017
2τ		407		50.5	44.6	43.6	35.3	32.8	30.7	26.2	21.6	16.1	24.1	11.5	6.8
$C_T(90°)\cdot f$	12.30	1500	527	1630	1990	1864	1480	1380	1330	1132	973	815	1066	515	289
"	12.75	1490	683	1675	1940	1920	1510	1430	1288	1145	920	657	985	457	227
"	11.70	1500	612	1750	2032	2010	1580	1378	1350	1116	927	660	907	445	209
$C_T(180°)\cdot f$	13.20	1141	482	1345	1664	1600	1205	1052	983	835	648	475	674	277	143
"	11.50	1148	565	1408	1746	1606	1166	1153	1023	804	646	437	618	252	150
"	12.75	1162	508	1340	1645	1587	1204	1114	1108	833	666	471	683	319	183
"	12.30	1167	531	1452	1658	1502	1180	1071	946	800	709	524	675	301	167
"	12.00	1154	570	1389	1648	1620	1180	1035	1032	819	665	458	654	331	163
$\bar{C}_T(90°)\cdot f$	(Average)			1685	1987	1931	1523	1396	1323	1132	940	711	986	472	242
$\bar{C}_T(180°)\cdot f$	(")			1387	1668	1583	1227	1085	1018	818	667	473	661	296	155
$-\bar{\bar{a}}(E)$				0.177	0.160	0.180	0.194	0.223	0.230	0.277	0.290	0.334	0.330	0.372	0.362
$-\bar{a}(E)$				0.193	0.170	0.190	0.215	0.245	0.255	0.316	0.337	0.371	0.393	0.424	0.420
S.D. $\pm$				0.015	0.016	0.017	0.017	0.017	0.019	0.021	0.024	0.026	0.023	0.028	0.038
$-a(E)$				0.201	0.176	0.200	0.224	0.256	0.276	0.330	0.351	0.387	0.409	0.442	0.437
γ-Spectrum		1.0		0.110	0.101	0.099	0.089	0.083	0.083	0.076	0.060	0.044	0.057	0.022	0.013
2τ		407		45.0	40.8	40.5	36.3	33.8	34.0	31.0	24.4	17.9	23.5	9.1	5.5
$\bar{C}_{T\gamma}(90°)\cdot f$				1783	1990	2159	1696	1762	1686	1549	1263	929	1139	418	238
$\bar{C}_{T\gamma}(180°)\cdot f$				1541	1778	1726	1531	1512	1453	1380	1114	712	1047	381	219
D				0.181	0.171	0.191	0.190	0.216	0.218	0.234	0.230	0.223	0.197	0.152	0.169
$-P_\gamma$				0.136	0.111	0.200	0.098	0.142	0.138	0.109	0.118	0.220	0.081	0.089	0.080

As an example take the first 12.3 hr. run at 90°, for which $F = 0.99$. The number of true coincidence counts received in channel 1 was:

$$\frac{163.0}{0.99 \times 527} \times 10^4 = 3125,$$

while the number of accidental coincidence counts was

$$\frac{50.5}{527} \times 10^4 = 950.$$

The standard deviations are calculated following the procedure in Appendices IV and VII.

APPENDIX VII.

CALCULATION OF STANDARD DEVIATION IN THE BETA-GAMMA CORRELATION COEFFICIENT.

From Appendix VI we obtain for the correlation coefficient:

$$\bar{a} = \bar{\bar{a}} \cdot \frac{1}{1-D} - P_\gamma \cdot \frac{D}{1-D}$$

Let this be written

$$\bar{a} = \bar{\bar{a}} \cdot b - P_\gamma \cdot Q .$$

then the deviation $\Delta \bar{a}$ is given by :

$$(\Delta \bar{a})^2 = (\bar{\bar{a}} \cdot \Delta b)^2 + (b \Delta \bar{\bar{a}})^2 + (P_\gamma \Delta Q)^2 + (Q \Delta P_\gamma)^2$$

The most important term is $(b \Delta \bar{\bar{a}})^2$ since it involves the error in the main experimental quantity $\bar{\bar{a}}$. Of the other terms only $(Q \Delta P_\gamma)$ is important since the remaining two both involve ΔD which is quite small. Therefore we obtain in sufficiently close approximation for the standard deviation in $\bar{a}$:

$$(\Delta \bar{a})^2 = (b \Delta \bar{\bar{a}})^2 + (Q \Delta P_\gamma)^2 .$$

APPENDIX VIII

CALCULATION OF a FROM a(E)

Let N(E) dE represent the beta spectrum, that is the number of beta particles whose energy lies between E and E + dE. The relation between the differential beta gamma correlation function W(θ,E) and the integrated correlation function W(θ) is then as follows:

$$W(\theta) = \frac{\int w(\theta,E)\, N(E)\, dE}{\int N(E)\, dE}$$

For Sb^{124} W(θE) is of the form:

$$W(\theta,E) = 1 + a(E)\cos^2\theta$$

where a(E) is the differential correlation coefficient. We have assumed W(θ,E) to be a probability, so it may be normalized as follows: $\iint W(\theta,E)\, d\Omega = 1$ where $d\Omega$ is a solid angle element. Consequently we have:

$$W(\theta,E) = \frac{1 + a(E)\cos^2\theta}{\int (1 + a(E)\cos^2\theta)\, d\Omega}$$, or after performing the integration:

$$W(\theta E) = \frac{3}{4\pi}\,\frac{1 + a(E)\cos^2\theta}{3 + a(E)}$$

Hence we may obtain W(θ) as follows:

$$W(\theta) = \frac{3}{4\pi \int N(E)\, dE}\left[\int \frac{N(E)}{3 + a(E)}\, dE + \cos^2\theta \int \frac{a(E)\, N(E)}{3 + a(E)}\, dE\right].$$

By analogy with the equation for W(θ):

$$W(\theta) \sim 1 + a\cos^2\theta,$$ we obtain:

$$a = \frac{\int_{E_{min}}^{E_o} \frac{a(E)\, N(E)}{3 + a(E)}\, dE}{\int_{E_{min}}^{E_o} \frac{N(E)}{3 + a(E)}\, dE} .$$

The range of integration extends from some minimum energy, E_{min}, (corresponding to the beta counter cutoff) to the maximum beta energy E_o.

APPENDIX IX.

EVALUATION OF THEORETICAL BETA-GAMMA-ANGULAR CORRELATION COEFFICIENTS.

The theory of Falkoff and Uhlenbeck (23) was used to predict the value of the correlation coefficient $a(E_o)$ for each of the possible transition schemes listed in Section VIII. Referring to (23) it is necessary first to specify the angular distribution function, $F_L^M(\theta, W)$, for the required interaction, and then to evaluate the parameters involved for the particular beta energy involved. For the axial vector interaction, first forbidden transition with matrix element B_{ij}, we have:

$$F_2^{\circ}(\theta, W) = \frac{1}{3}(2p^2 + 4q^2) + 2p^2\cos^2\theta$$

$$= \mu_1 + \cos^2\theta + \mu_2 \cos^4\theta .$$

giving $\mu_1 = (p^2+2q^2)/3p^2$ and $\mu_2 = 0$, where W is the total beta energy (in units mc^2), W_0 is the maximum beta energy and $q = W_0 - W$, $p^2 = W^2 - 1$. It is now possible to evaluate the parameter $\phi_{21}(\mu_1, \mu_2; \Lambda)$ from Equation (31) (15). The differential correlation function in this case is $W(\theta,E) = 1 + R/Q \cos^2\theta$ where $a(E) = \frac{R}{Q}$. $\frac{R}{Q}$ is given by Equation (29) (15), and may easily be evaluated from the partial sums listed in Table IV (15) or the sums in Table II (15).

As an example take the transition

$$1 \longrightarrow 1 \longrightarrow 0 , \qquad L_1 = 2 \qquad L_2 = 1$$

In Falkoff and Uhlenbeck's notation this is written :

$$J - \Delta j \longrightarrow J \longrightarrow J + \Delta J.$$

so that $\Delta j = 0$, $\Delta J = -1$, and $J = 1$.

The parameter $\mu_1 = \frac{1}{3}$ for $W = W_0$

Then $\phi_{21}(\mu_1, \mu_2 \Lambda) = \frac{1}{7}(10\mu_1 + 1) = \frac{13}{21}$; $\mu_2 = 0$, $\Lambda = 1$.

Referring to Table II (15) and equation (29)(15) :

$$R/Q = \frac{(2J-3)(2J+5)}{14J(2J-1)\phi_{21} + (8J^2 - 6J + 5)} = \frac{-1}{2\phi_{21} + 1}$$

$$= -0.447.$$

Similarly the other possibilities are evaluated, the results being listed in Table VI.

ELECTRONIC CIRCUITS

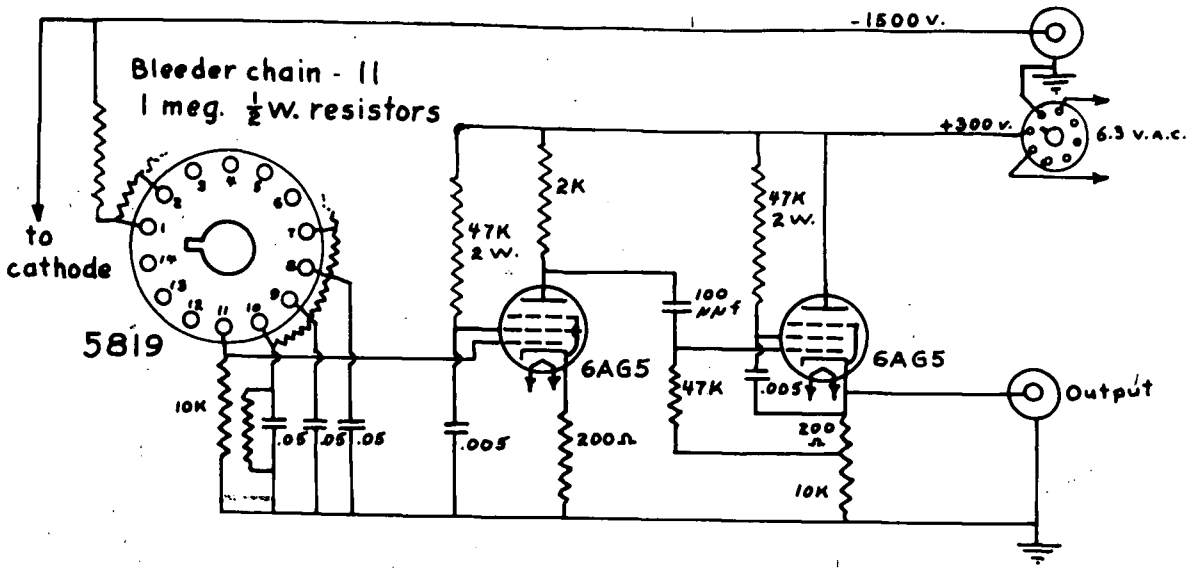

Preamplifier for Photo-multiplier

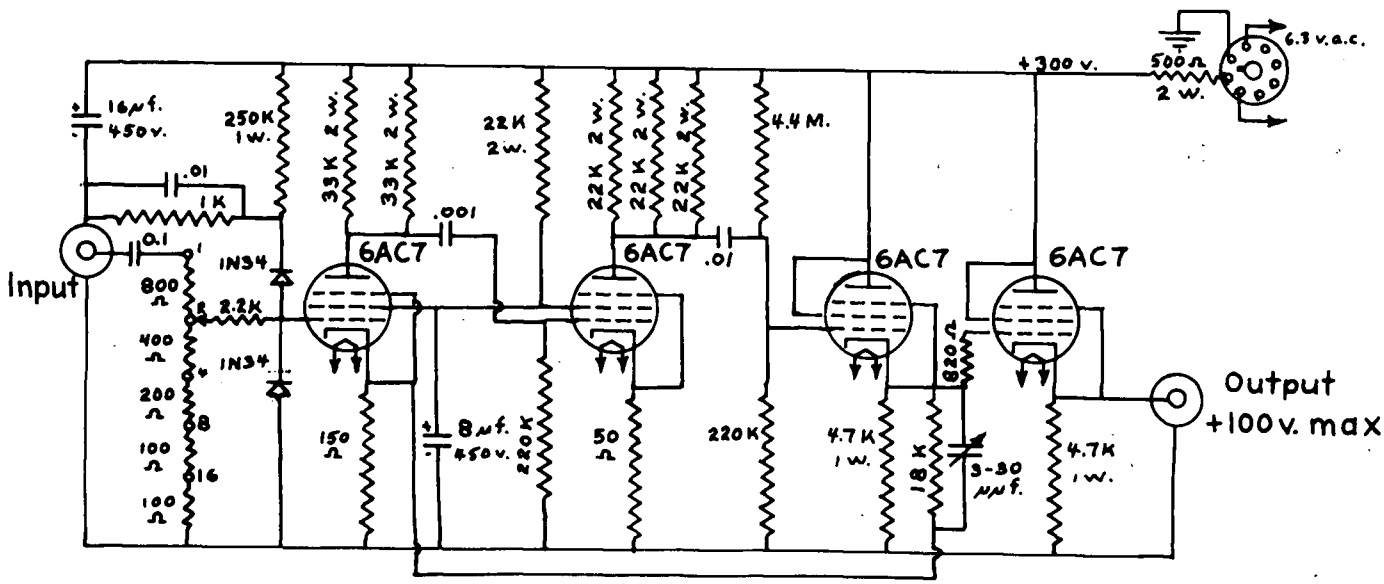

Linear Amplifier 100 X

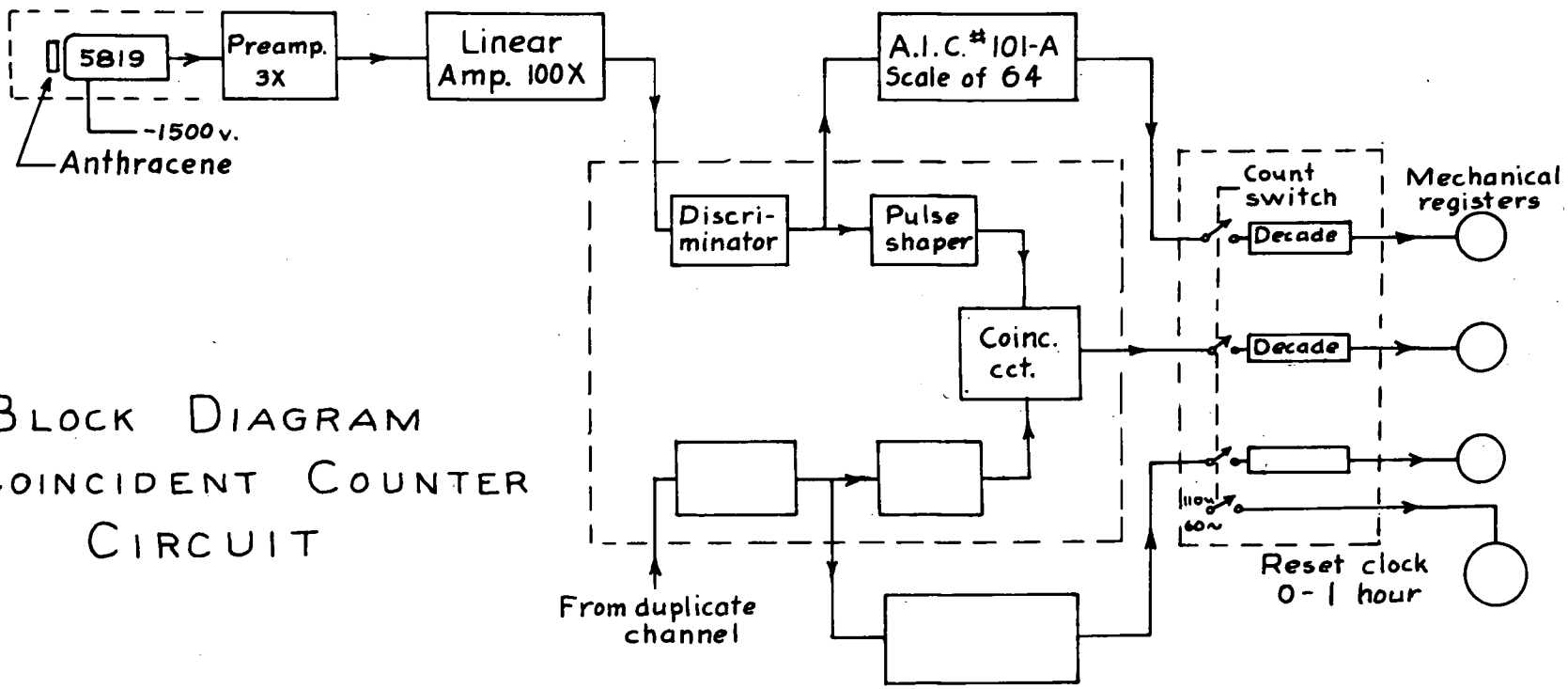

Block Diagram of Coincident Counter Circuit

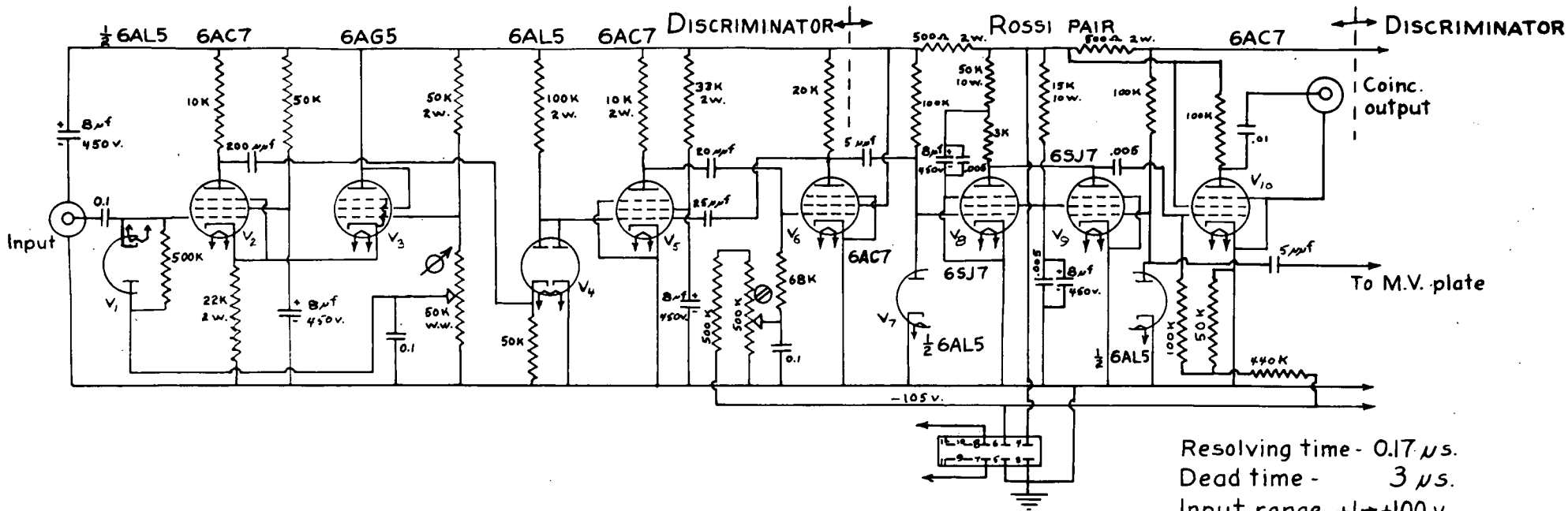

Resolving time - 0.17 μs.
Dead time - 3 μs.
Input range - +1 → +100 v.

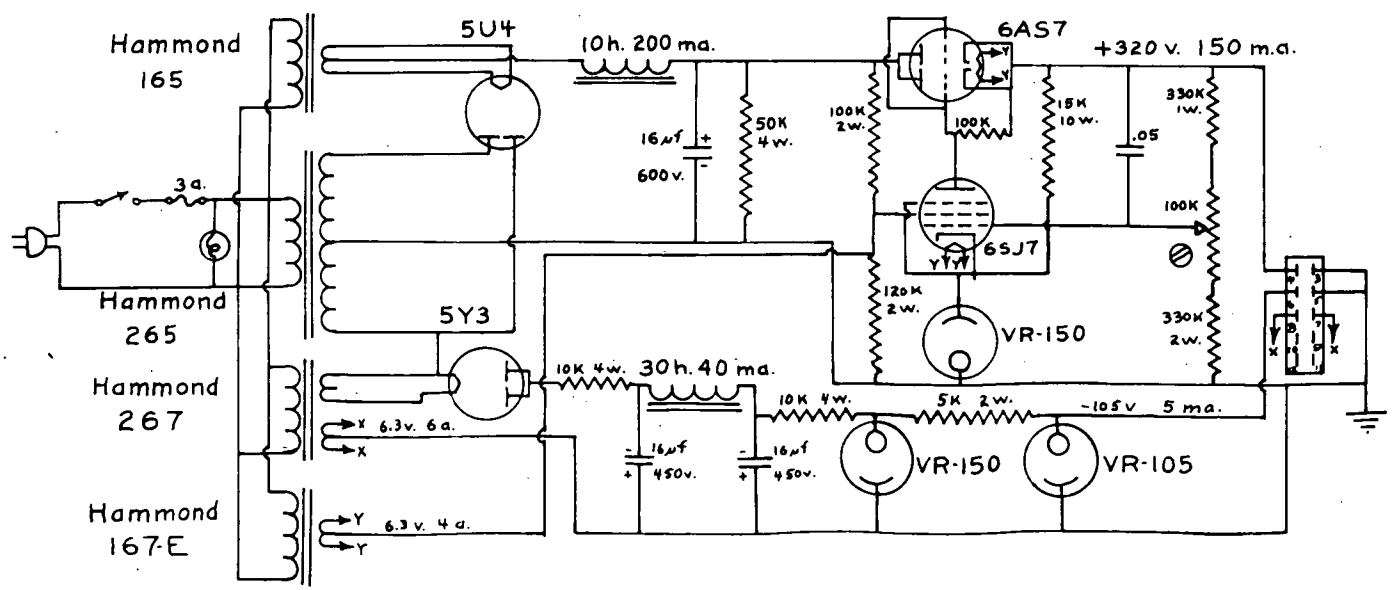

Coincidence Mixer and Power Supply

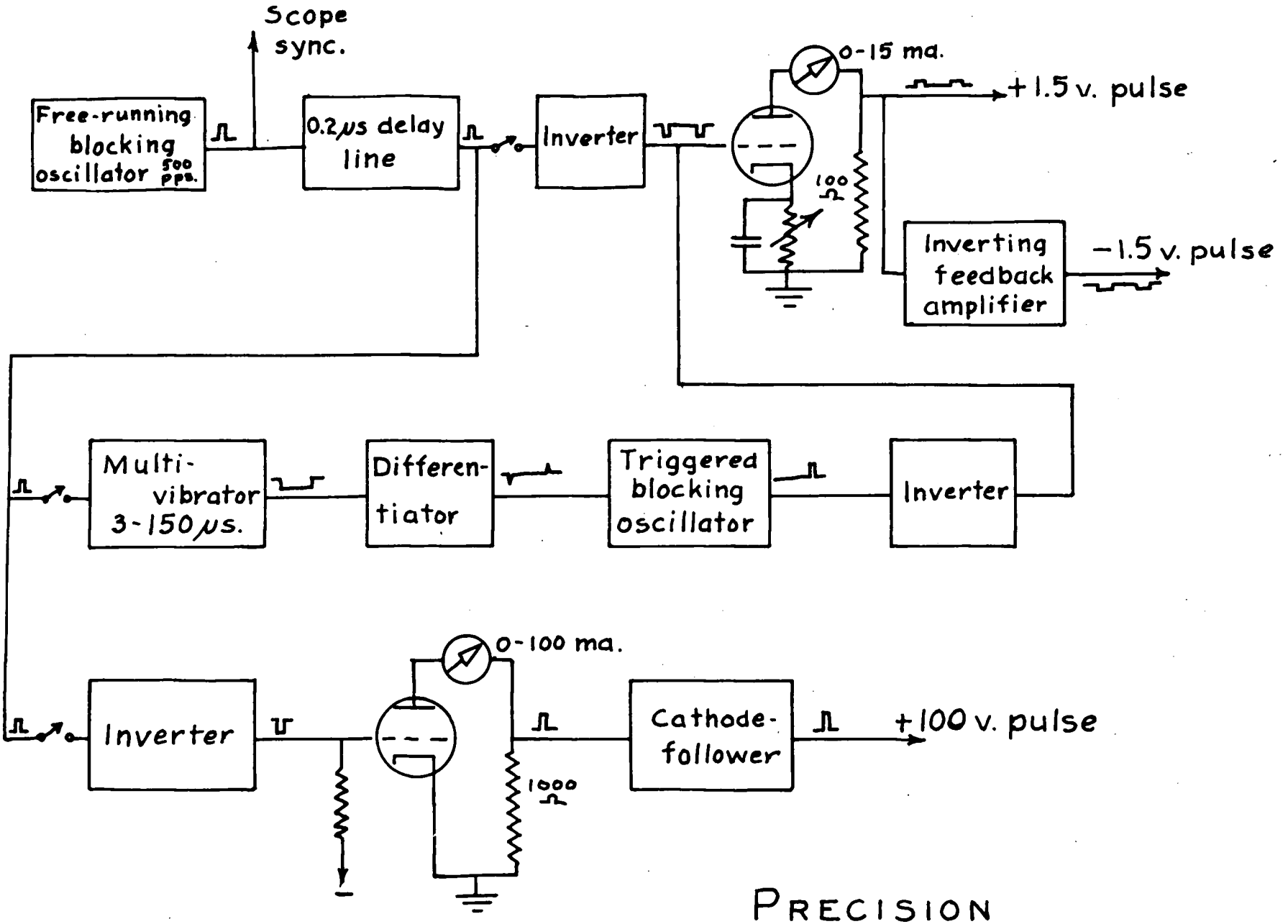

PRECISION PULSE GENERATOR

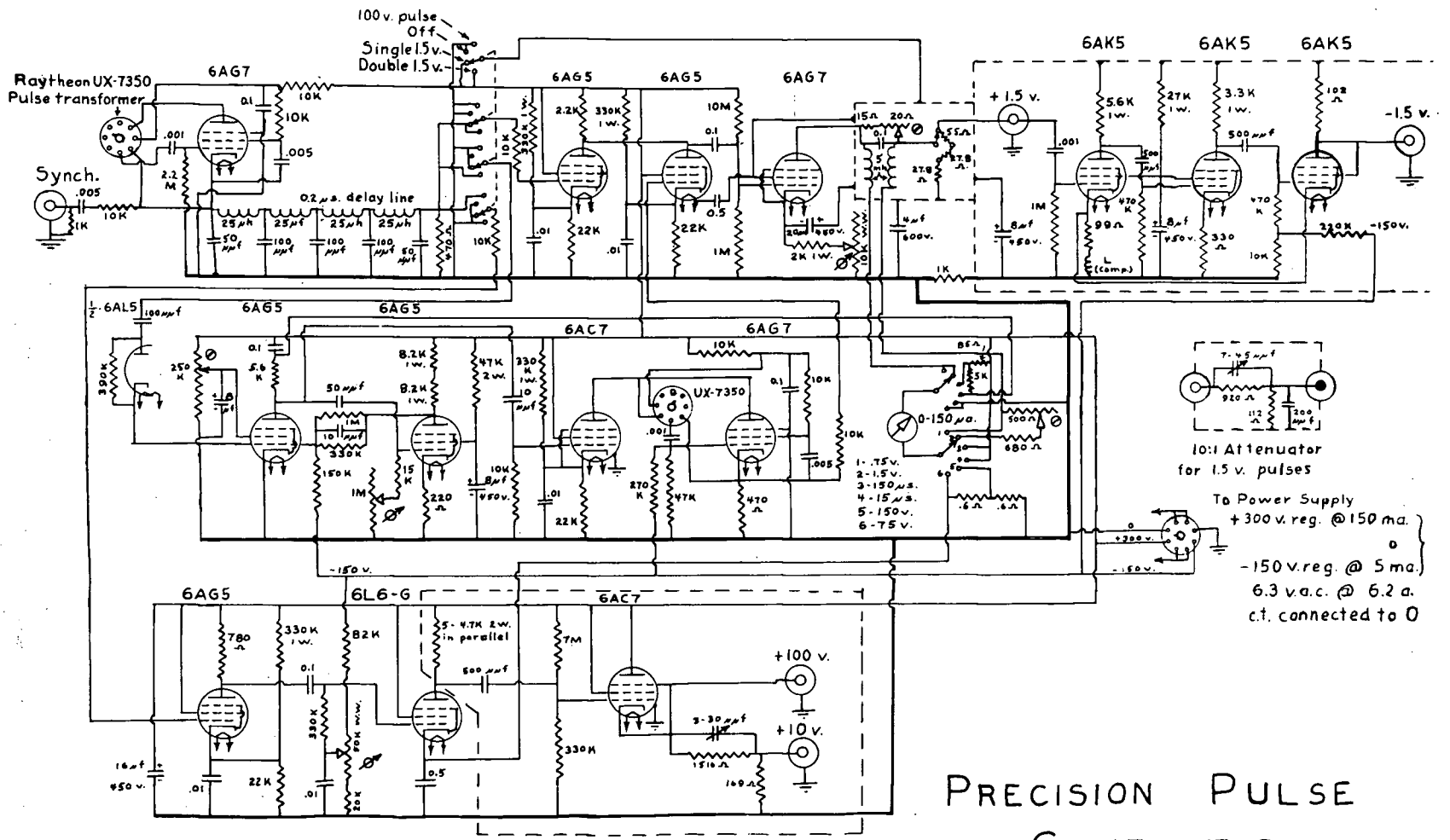

PRECISION PULSE GENERATOR

APPENDIX XI

ON THE INFLUENCE OF ABSORPTION ON THE MEASURED VALUE OF a *

The measurement of the integrated correlation function was important in that it was shown that no appreciable term in $\cos^4\theta$ exists. However the problem of comparing the measured integrated correlation coefficient with theory is quite complicated, due to the fact that the true beta spectrum is somewhat distorted by the aluminum absorber used to remove the lower energy beta particles. It is sometimes assumed (31) that beta particles of energy E are transmitted through aluminum according to a law of the form:

$$A = 1 - \frac{R}{R_{max}} \qquad (1)$$

where A is the transmission, R is the thickness of aluminum and R_{max} corresponds to the maximum range of beta particles of energy E. R_{max} and E are given by Feather's relation which has been improved by Glendenin (31):

$$R_{max} = 0.542E - 0.133$$

where R is in g/cm^2 and E is in Mev. ($E > 0.8$ Mev).

If the above relations are assumed, it may be possible to take the distortion of the beta spectrum into account and so obtain a suitable comparison with theory.

We may, however, check the consistency of the integrated and differential correlation measurements by estimating the

---

* I would like to thank Dr. L. Katz for bringing to my attention some aspects of the problems discussed in this appendix.

integrated correlation coefficient $\underline{a}$ from a(E) as shown in Appendix VIII, but applying a correction to N(E) on the assumption that beta particles in a small energy range, E to E+dE, are transmitted according to the above relation (1). In this manner we obtain the value, $a = -0.27 \pm 0.02$.

There is some evidence (29)(30) that the linear relationship as given in equation (1) for the transmission of an absorber is a rather poor approximation. The transmission in our experimental set up is undoubtedly considerably greater than is indicated by equation (1). This fact was checked by performing a measurement using an absorber of 440 mg/cm^2 of Aluminum, which corresponds to the maximum range of beta particles of energy E_c 1.06 Mev. The total absorbing thickness* used in the experiment was 310 mg/cm^2 corresponding to $E_c = 0.82$ Mev. The ratio K of the counting rate with $E_c = 1.06$ Mev to the counting rate with $E_c = 0.82$ Mev. was $K = 0.55$. If we assume that the absorber stops all beta particles with energy below E_c and transmits all beta particles with energy greater than E_c (i.e. ideal cut off) we may integrate the spectrum N(E) from E_c to E_o and thus obtain for the above ratio, the value $K = 0.65$. On the other hand, if we assume that the transmission is given by equation (1), we may perform the integration : $\int_{E_c}^{E_o} A(E)\, N(E)\, dE$, and estimate the ratio K. In this way we obtain the value $K = 0.48$.

It is apparent that the actual transmission is greater than that given by equation (1), but is of course less than the ideal

* In order to be counted, a beta particle had to penetrate the absorber, the counter window, and the counter crystal, which totaled 310 mg/cm^2.

transmission. Therefore our estimate of the measured integrated correlation coefficient $\underline{a}$ as obtained from $a(E)$ gives the result that $\underline{a}$ must lie between the values: $a = -0.24 \pm 0.02$ and $a = -0.27 \pm 0.02$. The value $a = -0.23 \pm 0.01$ is actually measured and deviates from the above estimate by about ± 0.02 to ± 0.03.

REFERENCES*

1. J. V. Dunworth, R.S.I. 11, 167 (1940).
2. D. R. Hamilton, P.R. 58, 122 (1940).
3. R. Beringer, P.R. 63, 23 (1943).
4. W. M. Good, P.R. 70, 978 (1948).
5. E. L. Brady and M. Deutsch, P.R. 74, 1541 (1948).
6. R. L. Garwin, P.R. 76, 1876 (1949).
7. J. R. Beyster and M. L. Wiedenbeck, P.R. 79, 411 (1950).
8. R. M. Steffen, P.R. 80, 115 (1950).
9. G. Goertzel, P.R. 70, 897 (1946).
10. D. S. Ling and D. L. Falkoff, P.R. 76, 1639 (1949).
11. S. L. Ridgway, P.R. 78 (821) (1950).
12. J. R. Beyster and M. L. Wiedenbeck, P.R. 79, 176 (1950).
13. D. T. Stevenson and M. Deutsch, P.R. 78 (640) (1950).
14. T. B. Novey, P.R. 78, 66 (1950).
15. D. L. Falkoff and G.E. Uhlenbeck, P.R. 79, 323 (1950).
16. E. K. Darby and W. Opechowski, P.R. 676 (1951)
17. E. K. Darby, Can. J. Phys. 29, 569 (1951).
18. D. T. Stevenson and M. Deutsch, P.R. 83, 1202 (1951).
19. S. P. Lloyd, P.R. 83, 716 (1951).
20. P. G. Hess, in print, Can. J. Phys.
21. U. S. National Bureau of Standards, Circular 499.
22. H. Frauenfelder, P.R. 82, 549 (1951).
23. D. L. Falkoff and G. E. Uhlenbeck, P.R. 79, 334 (1950).
24. M. Fuchs and E. S. Lennox, P.R. 79, 221 (1950).
25. J. I. Hopkins, R.S.I. 22, 29 (1951).
26. L. M. Langer et al, P.R. 79, 808 (1950).

27. S. Nakanawa et al, P.R. 83, 1273 (1951).

28. J. R. Beyster and M. L. Wiedenbeck, P.R. 79, 728 (1950).

29. J. S. Marshall and A. C. Ward, Can. Jr. Research A (15,39(1937)).

30. Rutherford, Chadwick and Ellis, Radiations from Radioactive Substances, Cambridge University Press, p. 414.

31. L. E. Glendenin, Nucleonics 2, 12 (1948).

* The following abbreviations have been used:

Physical Review: P.R.

Review of Scientific Instruments: R.S.I.